Preferred citation: R.W. Gooding, R.J. Kerekes and M. Salcudean. The Flow Resistance of Slotted Apertures in Pulp Screens. In **The science of papermaking**, *Trans. of the XIIth Fund. Res. Symp. Oxford, 2001*, (C.F. Baker, ed.), pp 287–338, FRC, Manchester, 2018. DOI: 10.15376/frc.2001.1.287.

THE FLOW RESISTANCE OF SLOTTED APERTURES IN PULP SCREENS

R. W. Gooding[1], *R. J. Kerekes*[2] *and M. Salcudean*[3]

[1]Pulp and Paper Research Institute of Canada Montreal, Canada
Presently with CAE Forestry Systems, Pulp and Paper, Montreal, Canada
[2]Paprican and the Department of Chemical Engineering,
UBC Pulp and Paper Centre, University of British Columbia,
Vancouver, Canada
[3]Department of Mechanical Engineering,
University of British Columbia, Vancouver, Canada

ABSTRACT

Pulp screens remove fibre bundles, plastic specks and other oversize contaminants from pulp suspensions before the pulp is made into paper. Within the pulp screen is a screen cylinder that acceptable fibres pass through but oversize contaminants do not. Apertures in the screen cylinder are in the form of holes or slots, and their size is perhaps the most critical variable in screening. Smaller apertures increase the removal efficiency of contaminants, but also lead to a reduction in screen capacity.

The development of screen plate "contours" in the early 1980s led to a revolution in pulp screen design. By locating apertures within recesses on the screen plate surface, smaller, more efficient, apertures could be used without a significant loss in capacity. Various theories have been proposed to explain the action of these contours. It may be that contours increase the turbulence at the aperture entry, which fluidizes the pulp and clears fibres from the aperture. It may be that the contours streamline the flow through the aperture to reduce hydraulic resistance. Alternatively, con-

tours may alter the streamlines through the aperture to reduce the tendency for fibres to become immobilized at the slot entry, which is a precursor to blockage. What is clear is that understanding the action of the contours is critical to the full exploitation of this important development in screening technology.

The objectives of the present study were: (1) to create a framework for assessing the flow resistance of screen plate apertures; (2) to learn how aperture size, screen plate contours, fibre blockages and other factors of practical importance affect resistance; and (3) to develop a more fundamental understanding of what determines resistance, and how this knowledge could be used to increase screen performance.

Flow resistance was assessed using the non-dimensional pressure drop coefficient (K) across the screen plate, and K was studied by three methods. Computational fluid dynamics (CFD) was used to predict how aperture geometry and flow variables affect K in an idealized screening configuration. Experiments with a flow channel were used to confirm the theoretical CFD findings and explore how fibre accumulations at the screen aperture affect K. Finally, trials with an industrial pulp screen showed how industrial variables such as pulp consistency and pressure pulsations influence K.

CFD analysis determined that the vortex at the slot entry has a dominant influence on K for water flow. The size of the vortex was reduced by increasing the ratio of slot velocity to upstream velocity, a quantity termed the “velocity ratio” (V_N). The relationship between K and V_N was defined by two regimes: a “descending regime”, where K decreased rapidly with increased V_N, and a “constant regime” where K was relatively independent of V_N. Examination of the flow patterns revealed that for smooth slots, the vortex on the upstream side of the slot diminished in size in the diminishing regime. The flow then approached a pattern that was relatively unaffected by further increases in V_N (constant regime). The presence of a contour at the slot entry led to the expected reduction in K. This study showed that the effect of the contour is dependent on V_N. At low values of V_N, the contour actually caused K to exceed the value for a smooth slot. The precise dimensions of the contour are critical to its effect. For a step-step type of contour and $V_N = 0.5$, the optimal contour for simple hydraulic resistance had a depth of 0.25 mm and step-width of 0.50 mm. An increase in the contour depth to 1.0 mm caused K to double and to exceed the value for when there was no contour at all.

Experimental measurements of K were made for steady flow through slots in a plexiglas channel. Good agreement with the CFD findings was obtained for both smooth and contour slots. To assess the influence of fibre accumulations, the instantaneous value of K was monitored as a fibre accumulation grew. In one typical case, a fibre accumulation filled half of the slot width and caused K to increase from 4.3 to 9.8. This finding underlines that flow resistance is due to both the hydraulic resistance of the slot and the added resistance due to fibre accumulations within the slot.

Pilot plant tests were conducted to assess K in an industrial-scale pulp screen. The screen was modelled as a series of resistances combined with the pumping effect of the rotor. One could thus infer the resistance of the screen apertures by measuring the overall pressure differential across the pulp screen, and then by discounting the influences of the screen rotor and housing. The findings for water flows were in agreement with the CFD and flow channel work: The descending-constant form of the K-V_N relationship was again found, and the values of K were comparable to those in the CFD and flow channel work. The use of a 1.5% pulp suspension instead of water caused K to double in one typical case, indicating substantial accumulation of fibre within the slots.

This study has defined K as the essential measure of flow resistance and shown how it can be measured through theoretical, flow channel or pilot plant tests. The value of K was found to depend on both hydraulic resistance and the degree of fibre blockage in the screen slot. Screen plate contours were found to reduce K by streamlining the flow, although it is recognized that they may also reduce the tendency for fibres to accumulate within the slot. Values of K can thus be used in the development of improved screening technology, and to compare the performance of screen cylinders from different suppliers. The use of K is also important for process control routines that estimate the extent of fibre blockages in screen plate apertures and act to prevent screen failure.

INTRODUCTION

Pulp screens remove fibre bundles, plastic specks and other oversize contaminants from pulp suspensions before pulp is made into paper. These contaminants might otherwise appear as dirt in paper, reduce paper strength, or lead to operating problems such as coating streaks and paper breaks. The removal of these contaminants is essential for the efficient production of high-value grades of paper. Current trends in the pulp and paper industry are making screens even more important. Paper recycling has increased the quantity and variety of contaminants in pulp. Environmentally-attractive, non-chlorine bleaching processes are typically less effective for the removal of fibre bundles. Globalization of the pulp and paper markets has increased the competitive pressure to provide a high-quality, contaminant-free product. Moreover the drive to develop new paper products has increased interest in fibre fractionation, which is the separation of fibres of differing size and flexibility. Pulp screens are finding increased use in these various applications.

The most common type of pulp screen is the pressure screen, which was considered exclusively in this study. The key components of a pulp screen are the screen cylinder and rotor. The cylinder has apertures which allow the passage of the accept pulp, but not the oversize contaminants. The rotor causes pressure pulsations which backflush the screen plate apertures and clear away any accumulations of pulp fibres. It also accelerates the pulp on the feed side of the screen to a high tangential velocity, and induces turbulence at the surface of the screen plate – factors important to screen performance. The apertures in the screen cylinder may be in the form of holes or slots. They can present a physical barrier to the contaminants (termed “barrier screening”) or create a flow field at the aperture entry that restricts the passage of contaminants (“probability screening”). The size of the apertures is perhaps the most critical variable in pulp screening. Smaller apertures will increase the removal efficiency of contaminants, but will typically lead to a reduction in screen capacity.

The development of screen plate “contours” in the early 1980s led to a revolution in pulp screen design. By locating apertures within recesses on the screen plate surface, smaller, more efficient, apertures could be used without a significant loss in capacity. The general designation of a “contour” slot refers to any slot with a recess at the slot entry and embraces a range of products that have been developed by various suppliers. Traditional screen slots, which have no protrusions or depressions, have come to be called “smooth” screen plates. Various theories have been proposed to explain the action of these contours. It may be that contours increase the local turbulence at the aperture entry, which fluidizes the pulp and clears fibres from the aperture. It may be that the contours streamline the flow through the aperture to reduce hydraulic resistance. Alternatively, contours may alter the streamlines through the aperture to reduce the tendency for fibres to become immobilized at the slot entry, which is a precursor to blockage. A more complete understanding of the action of the contours is required to support the full exploitation of this important development in screening technology.

The objectives of the present study were: (1) to create a framework for understanding the flow resistance of screen plate apertures; (2) to learn how aperture size, screen plate contours, fibre blockages and other factors of practical importance affect resistance; and (3) to develop a more fundamental understanding of what determines resistance, and how this knowledge could be used to increase screen performance. Three complementary lines of study were followed to meet these objectives: computational fluid dynamics (CFD), flow channel experiments with a highly simplified screen configuration, and pilot plant trials with an industrial pulp screen.

LITERATURE REVIEW

The present study of the flow resistance of slots in pulp screens builds on several bodies of knowledge. A general understanding of flow resistance and the flow through apertures is available from the field of fluid mechanics. The pulp and paper literature provides some understanding of how fibre accumulations increase flow resistance, and how a screen rotor produces pulsations to backflush apertures. Other studies have considered how these effects affect overall pulp screen performance.

Flow through screen apertures

The performance of pulp screens and pulp screen systems is determined by what happens at the screen plate apertures. Flow through apertures has been studied in various engineering applications, such as the flow through wire meshes, perforated plates and nozzles. The flow through pulp screen slots differs significantly, however, from these more common situations. One main difference is that the flow in a pulp screen approaches the slot entry parallel to the screen plate rather than perpendicular to it due to the high tangential velocity induced by the rotor. The flow through an aperture in a pulp screen must therefore split from the mainstream flow parallel to the plate, creating a flow bifurcation, and turn to pass through the slot.

Relatively few studies have been made of a bifurcating/turning flow.

Thomas and Cornelius [1] conducted an experimental study of this flow using water as the medium and relatively low-speed (laminar) flows. Pressure drop was assessed using a non-dimensional, pressure drop coefficient, *K*:

$$K = \frac{\Delta p_S}{\frac{1}{2}\rho V_S^2} \tag{1}$$

where Δp_S is the difference between the pressure in the mainstream flow above the slot and that in the plenum below the slot, and V_S represents the mean velocity through the slot. Thomas and Cornelius identified the presence of a recirculating zone in the aperture on the upstream wall of the slot, just below the entry. They noted that both the value of *K* and the size of the recirculating zone increased with increased upstream velocity or reduced slot velocity.

The flow through slots in pulp screens includes the additional complexity of the contours on the feed side of the slot. These contours have enabled smaller apertures to be used in screening without sacrificing screen capacity. In the early 1960s, a typical screen aperture was a 1.8 mm diameter hole. These efficiently removed long fibre bundles, but were much less effective for the removal of cubical debris. Screen plates with slots, typically with slot widths less than 0.5 mm, were required to remove cubical debris but their low capacity limited their use. In the early 1980s, contoured screen plates were introduced [2–4] and a few of the various commercial designs of these contours are illustrated in Figure 1. The dramatic increase in the capacity of contour screen plates led to an increase in the number of installations where slotted screen plates were used. The increase in capacity associated with the use of contour plates has often been ascribed to turbulence caused by the contour, but there has been no rigorous, scientific study of the action of the contour. What was clear was that this design of screen plate could provide good capacities with a slot width as small as 0.10 mm, and thus ensure a high degree of contaminant removal for both cubical debris and fibre bundles. There are continued efforts to reduce the slot width until it approaches the diameter of pulp fibres (~0.04 mm).

Some studies of the flow through apertures have been modelled on the flows in pulp screens. Oosthuizen et al. [5] confirmed the existence of an exit layer that turned from the upstream flow and passed into a smooth slot. Halonen et al. [6] studied a turbulent slot flow theoretically using CFD. They mapped the flow patterns found in the contour and slot entry region, and Figure 2 shows some of their results. Of particular note is the recirculating zone on the upstream edge of the slot in the smooth screen plate. The pres-

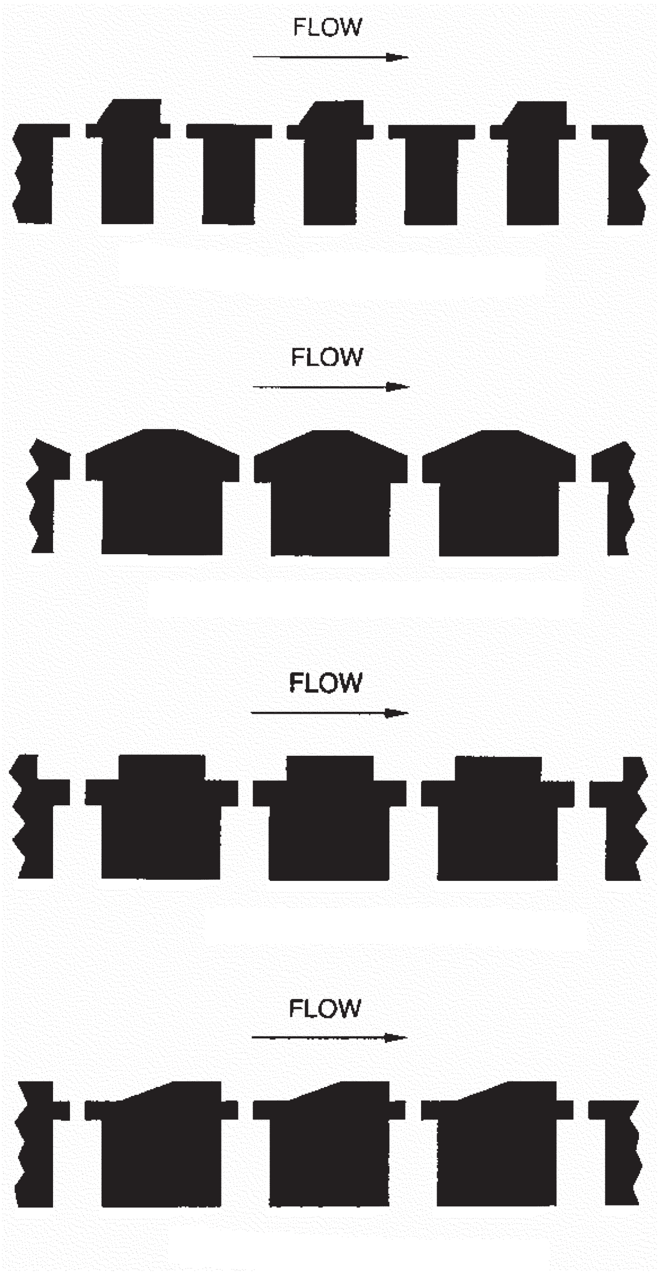

Figure 1 Some commercial contour designs. Drawings are not to scale.

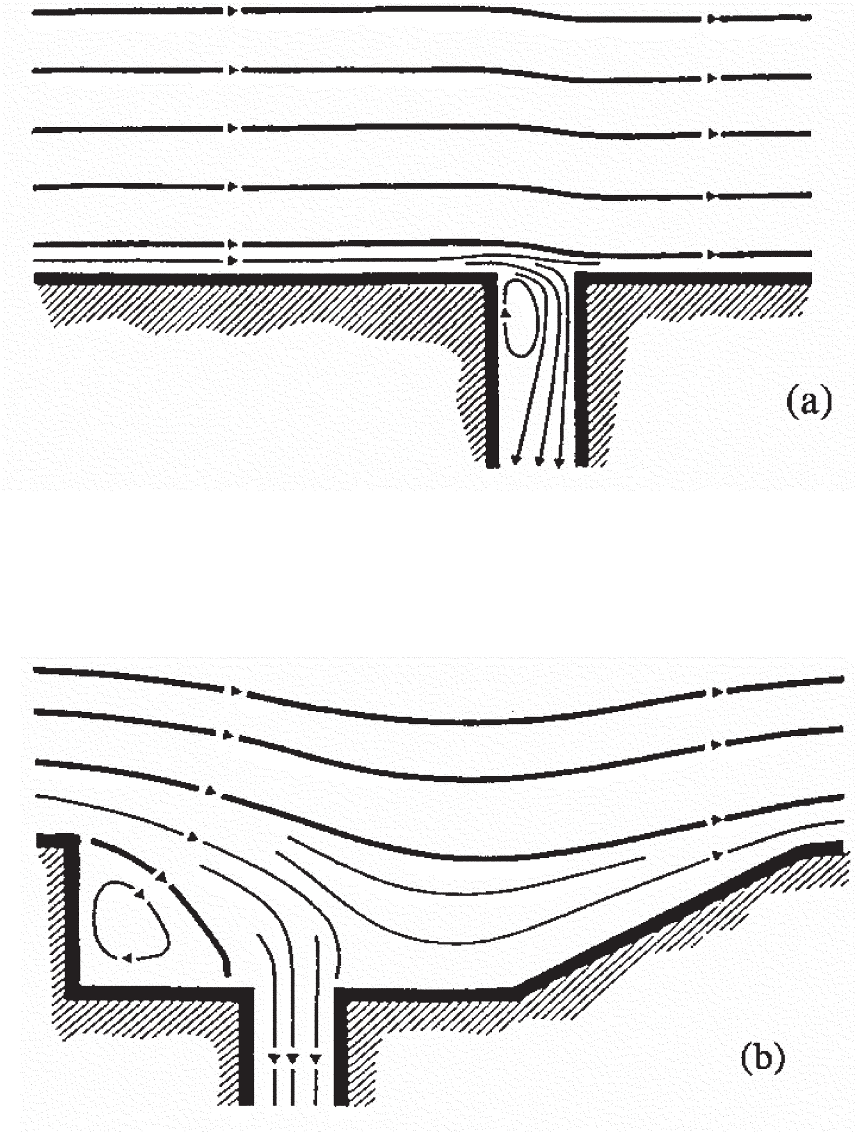

Figure 2 Flow patterns in a smooth slot (a) and contour slot (b) [6].

ence of a contour caused the recirculating zone in the slot to disappear, and the level of turbulence at the slot entrance to increase. Gunther [7], Yu and Defoe [8], and Tangsaghasaksri [9] analyzed smooth and contour slots using CFD. All showed that contours cause the elimination of the vortex within the slot. Their work was focused, however, on the evaluation of particular contour geometries rather than on a detailed understanding of how flow structures contribute to hydraulic resistance. None of the above studies included the necessary, detailed information that would allow the CFD methodology to be evaluated. Moreover, while several studies have compared contour shapes that differ greatly in shape, none has examined a generic contour shape and considered how its dimensions affect flow patterns and hydraulic resistance.

The flow resistance of screen plates in pulp screens has also received little attention in the literature. Yu et al. [10] proposed that the effective resistance of a screen plate can be considered as the product of several factors. The first is the intrinsic resistance of the aperture. Next is a rotor factor, which accounts for the flow reversals that occur during pulsations. A third factor reflects the size of fibre accumulations that form in the screen plate apertures. Finally, a pulp factor represents the strength of the pulp flocs, recognizing that stronger flocs would resist disruption and be more likely to block the apertures. The paper did not give a detailed analysis of each factor, but the listing of factors was a useful step forward. Tangsaghasaksri [9] measured pressure drop in a screening channel for various contours and flow conditions, but did not measure the associated local velocities. Inferences of pressure loss and flow resistance were not possible because the pressure drop resulting simply from velocity changes (i.e., the exchange of pressure energy and kinetic energy) was unknown.

Fibre accumulations and rotor effects

The presence of pulp fibres adds an additional level of complexity to the flow through apertures in pulp screens. Fibres can accumulate within screen apertures and, in the extreme, cause blinding. Using high-speed cine-photography, Gooding and Kerekes [11] observed how fibres may become immobilized on the downstream edge of a slot in an idealized screening channel. Using a very similar apparatus, Kumar [12] classified the flow conditions that cause these accumulations of fibres to grow. In both of these tests, steady flow and very dilute suspensions were used. Julien Saint Amand and Perrin [13] have developed a theoretical model that considers the accumulation of fibres within the slot and some of the dynamic aspects of fibre passage. Tests in industrial pressure screens have generally been limited to investigations of how elevated consistencies and insufficient pulsation from the rotor lead to blinding and screen failure.

The rotor plays a critical role in screen operation, and it has three main functions. Its most important function is to cause pressure pulsations which backflush and clear the screen plate apertures of any accumulated fibre. The rotor also induces turbulence, which is believed to disperse fibre flocs upstream of screen plate apertures, and release fibres trapped in the apertures. Finally, the rotor induces a tangential velocity in the feed-side flow approaching the screen apertures. The flow therefore approaches each aperture from along the screen plate surface and then turns sharply into the aperture. Both the approach flow and how it turns into the aperture have been found to play an important role in the mechanism of probability screening which restricts the passage of oversize debris [11].

There is a range of rotor designs available commercially. All have protuberances that pass within 1 to 3 mm of the screen, but do not contact or wipe the screen plate surface. The protuberances can be in the form of blades, foils [14–16], bumps [17], or a shaped rotor core [18–20], and tip speeds of the rotors are in the range of 10–40 m/s. Pulse frequency will naturally increase as the rotor speed is increased. Pulse strength will increase with rotor speed and as the clearance between the rotor and screen plate is reduced. Both of these effects will reduce the tendency for fibres to accumulate within screen apertures. However higher rotor speeds will cause an increase in power consumption, and stronger pulses may cause some oversize contaminants to pass through the screen plate apertures. Increased passage of contaminants is thought to occur because the stronger pressure pulses might force flexible contaminants through the aperture. Stronger pulses will also generate larger flow reversals. The instantaneous velocity between pulses will need to increase to compensate, and higher passing velocities will tend to cause the passage of contaminants to increase.

Despite its importance, only a few industrial studies have discussed the strength and form of pressure pulses induced by the motion of the rotor [14]. A useful study was made by Karvinen and Halonen [21] who assessed pressure pulsations using experimental and computational techniques for a foil-type rotor. They assumed that the flow induced by the rotor was turbulent, and found that the backflushing action of the pressure pulse arose from a Venturi effect created by the acceleration of the flow through the gap between the moving rotor tip and stationary screen plate. This acceleration causes the local pressure on the feed side of the screen plate to decrease to the point that the flow through the aperture reverses. The flow then passes from the accept side of the screen plate to the feed side, and releases any plugged fibres. A more recent study of the rotor action was made by Wikstrom and Fredriksson [22]. This study assumed the flow induced by the rotor was laminar, which contrasts with the turbulent assumption used by Halonen et al. Both studies, however, found good agreement with experimental measurements.

Pulp screen performance

Pulp screen performance is assessed in terms of removal efficiency (the percentage of contaminants removed) and screen capacity (the mass flow rate of accept pulp per square meter of screen plate surface area) [23–25]. Other important parameters are the screen motor load, reject consistency, minimum reject rate and equipment reliability. Variables like aperture size, rotor configuration and reject ratio have a predominant influence on performance and must be carefully selected for each particular application [26–28]. Aperture size is particularly critical since a small aperture will ensure the maximum removal of contaminants, but too small an aperture will reduce screen capacity below acceptable limits.

Accept flow and consistency measurements reflect capacity. The pressure differential between the feed and accept lines of a pulp screen gives a general indication of the flow resistance through the screen plate. Resistance increases rapidly when the screen plate becomes blinded with pulp, and pressure differential is routinely used for process control. When plugging is detected, the flow through the screen is stopped and flushing sequences are initiated to clear the screen plate before operation of the screen is resumed [29]. Hourula et al. [30] studied the feed-accept pressure differential under a range of hardware and operating conditions and identified: the strong pumping action of the rotor, the significant flow resistance of the screen housing, and how pressure loss increases with accept flow. Walmsley and Weeds [31] described how the feed-accept pressure loss increased with increased feed/reject flow (for a constant accept flow) and doubled when feed consistency increased from 0.6 to 1.4%. The former effect reflects the resistance of the screen housing. The consistency effect likely results from the increased obstruction of the slots with fibres. Torsten Paul et al. [32] modelled pressure drop across a pulp screen and proposed a pressure loss coefficient which followed on the form of equation 1. They found that factors that reduce fibre flocculation, such as an increase in viscosity, or a decrease in the disruptive shear stress of the pulp, reduced the feed-accept pressure loss across a screen. This suggests that flocs play a more important role than the individual fibres in obstructing slots and increasing flow resistance.

Martinez et al. [33] developed a model of screen capacity that combined the effects of hydraulic resistance and fibre blockages, and successfully tested the model with a range of screen cylinders in a pilot plant screen. The model showed that volumetric capacity could be expressed as a product of three factors: open area, hydraulic resistance and pulse/plug strength. This work provided an integrated understanding of the fundamentals of flow through an aperture, the effect of fibre accumulations on resistance and the capacity of industrial pulp screens.

The above literature reflects the growing appreciation for the importance of flow resistance and a knowledge of the underlying mechanisms. The need remains, however, for a more comprehensive understanding of resistance and its relationship to pulp screen operation.

CFD ANALYSIS

Computational fluid dynamics (CFD) provides a means of estimating the hydraulic resistance of a screen slot using theoretical, computer-based methods. Purely analytic methods are limited to very simple slot flows, such as laminar [34] or potential [35] flow through a smooth slot. Using CFD, one may consider more realistic conditions, such as the turbulent flow of fluids through slots with complex geometries. One can not only determine hydraulic resistance, but also details of the flow patterns and turbulence levels near the slot.

Procedure

The general approach in CFD is to divide the flow field into a grid of small cells and to calculate values for velocity, pressure, turbulent kinetic energy and turbulent kinetic energy dissipation rate for each cell which satisfy the conservation equations and boundary conditions for the flow field. The principles of CFD are discussed in standard texts [36–38]. Details on the approach used here and on tests of convergence and grid sensitivity are given in Gooding [39]. A commercial CFD code named INCA [40] was used in this work. INCA is based on a finite volume approach and for this study, a two-equation k-ε turbulence model was used with a low-Reynolds number approach for modelling the effect of the wall.

The problem defined for analysis with CFD was a flow bifurcation at a two-dimensional tee where the flow is steady, the presence of pulp is neglected, and the fluid is assumed to be Newtonian. This is vastly simplified relative to an industrial pulp screen, and many of the complicating factors have been omitted – such as the intricate three-dimensional shapes of the rotor and screen plate, the transient flows caused by the action of the rotor, and the complex rheology of a suspension of pulp fibres. The simplified

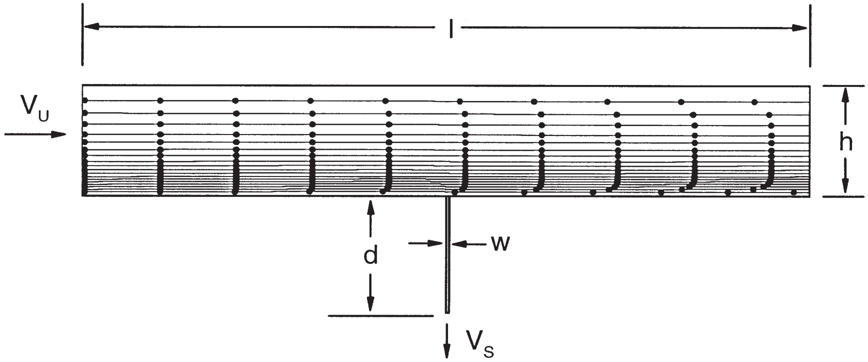

Figure 3 Flow field for a smooth screen slot with time markers on the streamlines.

problem could nonetheless provide some insight into what determines hydraulic resistance in screens, and serve as a basis for further studies.

The flow field used for CFD analysis of smooth slots is shown in Figure 3. The variables that define the field are: the channel length (*l*), channel height (*h*), slot width (*w*) and slot depth (*d*). A channel height of 19 mm was used throughout this analysis which corresponds to the distance between the rotor core and screen plate in one model of pulp screen. Other screens have larger values of *h*, but the general conclusions of this study are expected to be equally applicable to these screens. The values chosen for channel length and slot depth were 120 mm and 20 mm respectively. The boundary conditions for the channel and slot were: uniform total pressure across the inlet; constant static pressure across the channel outlet and at the slot discharge; and no-slip walls along the surfaces of the channel and slot. The boundary conditions for the exit flows require that the flows are "fully developed" and so values of *l* and *d* were chosen to ensure that disturbances introduced by the slot flow had sufficient time to disappear before the flow exited. The slot depth (*d*) required to achieve a fully-developed flow was several times greater than slot depths found in industrial screen plates, however the method used to assess resistance corrected for the extended length. Flow discharging from a slot in an industrial screen plate would be expected to have a very non-uniform flow/pressure profile.

Contour slots were also analyzed using CFD. A common industrial design is the Lehman contour, where the recess has a simple, rectangular shape, as shown in Figure 4. For convenience, the Lehman contour will be examined in

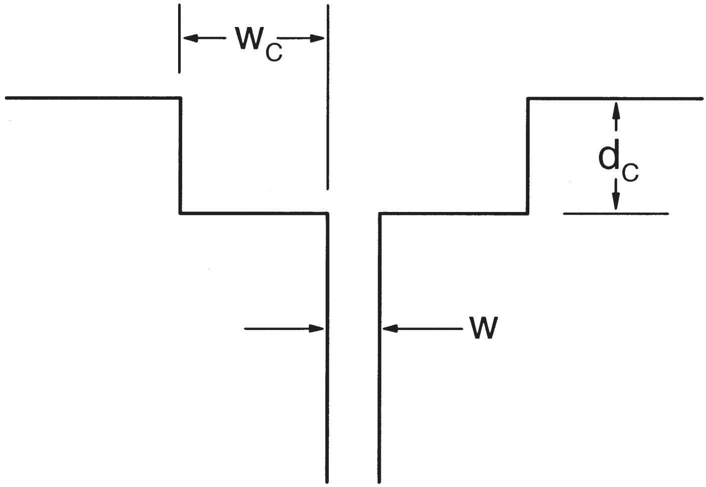

Figure 4 Step-step contour slot geometry.

this study, and designated as a "step-step" contour geometry. In particular, the analysis will focus on 0. 5 mm-wide slots that are centrally-located in the contour. The contour shape is described by two variables: contour depth (d_C) and contour step-width (w_C).

The Reynolds number (*Re*) for the channel flow was in the order of 10^6, which is well into the turbulent regime for a fully-developed pipe flow. The nature of the slot flow is not straightforward though. *Re* varied from 10^2 to 10^4 over the range of experiments, which indicates the flow could be laminar, turbulent, or transitional. Turbulent effects from the channel flow extend into the slot and the slot flow does not satisfy the requirements of a traditional k-ε model (i.e., isotropic, high-*Re*). The low-*Re* turbulence model used in this study may be more suitable but this has not been rigorously established. CFD solutions for the slot must be treated cautiously, especially for cases of low V_S.

To assess the pressure drop attributable to the slot entry, the steady one-dimensional energy equation was applied to the flow through the slot. This follows the methodology commonly used to assess pressure drop in piping systems [41], and details of this approach are given in Gooding [39]. This routine makes careful account of the transfer between kinetic energy and pressure, correction factors to account for velocity gradients, and energy losses that occur along the length of the channel and slot that are independent of the loss due to the slot itself. In an industrial pulp screen, the slot flow is discharged into a plenum and the kinetic energy of this flow dissipates as turbulence and is lost. The kinetic energy of the flow leaving the slot was added to the pressure loss at the slot entry determined by CFD to give an overall estimate of pressure loss due to the slot, Δp_S. The pressure drop coefficient was then determined using equation 1.

RESULTS

Smooth slots are rarely used in industry. Flow through a smooth slot can, however, be considered as a base case to which more complex flows will be compared. Flow/pressure solutions were determined for three upstream velocities ($V_U = 5$, 7.5 and 10 m/s) and slot velocities in the range of 0 to 9.5 m/s. The mean slot velocity in an industrial screen is typically in the range of 0.5 to 2 m/s. The instantaneous velocity will be somewhat greater, however, given the need to compensate for flow reversals induced by the rotor.

For a 0.5 mm wide slot, Δp_S was found to be strongly dependent on V_S. Figure 5 shows the rapid increase of Δp_S with increasing V_S. For a given V_S, larger values of V_U gave increased Δp_S. Plots of the above data are given in non-dimensional terms (i.e., K versus V_N) in Figure 6 where V_N is defined in equation 2. The data collapse onto a single curve.

$$V_N = \frac{V_S}{V_U} \tag{2}$$

Figure 6 indicates that the K-V_N relationship can be divided into two regimes. At low values of V_N, K decreases rapidly with increasing values of V_N. At higher values of V_N, however, K tends to a constant value – which in the case of this smooth slot is 1.8.

The effect of slot width was also assessed for smooth slots at constant V_U (7. 5 m/s). Table 1 shows that the effect is relatively small. A 400% increase in slot width (from 0.25 mm to 1.0 mm) increased K by only 24% at $V_N = 0.2$ ($V_S = 1.5$ m/s) and decreased K by 8% at the higher slot velocity. The choice of slot widths was based on industrial values. Both 0.25 and 0.5 mm wide slots are in common use, although it is recognized that there has been a trend to ever-smaller slot widths, and 0.15 mm slots are common. The 1.0 mm slot was included because it was used in the flow channel tests to observe fibre accumulations.

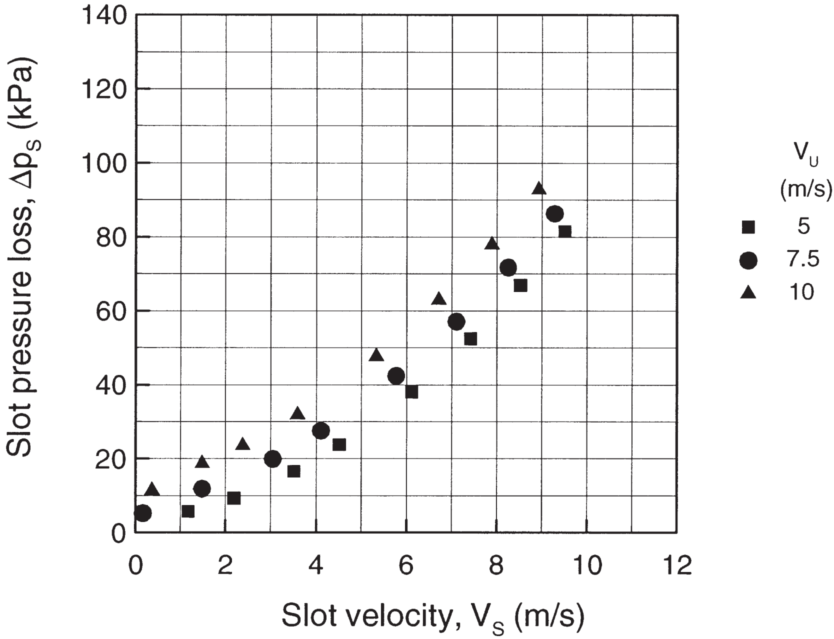

Figure 5 Pressure loss for a smooth slot for a range of upstream velocities (V_U).

Table 1 Effect of slot width on pressure drop coefficient (K).

V_N	K		
	0.25 mm	0.5 mm	1.0 mm
0.2	9.7	10.8	12.0
0.9	2.4	2.3	2.2

Pressure drop reflects the energy lost through viscous dissipation. Detailed flow patterns in the slot entry can identify the locations of high velocity gradients, the likely sites of dissipation, and hence the possible sources of K. Figure 7 presents flow patterns for the aperture in Figure 3 with $w = 0.5$ mm, $V_U = 7.5$ m/s, and V_S in the range of 0.2 m/s to 9.3 m/s. The flow patterns in Figure 7 are for V_U flowing from left to right. One key feature of the flow is

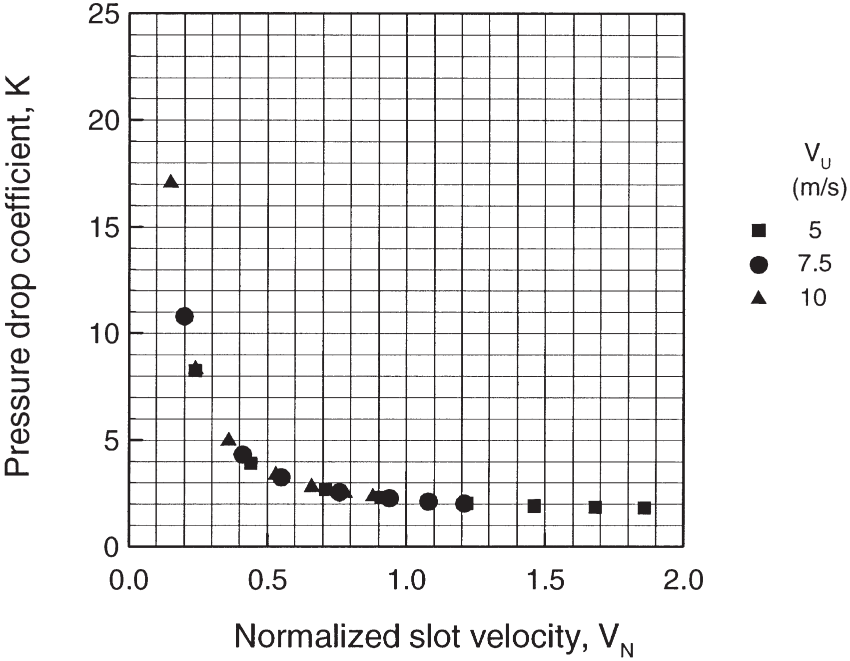

Figure 6 Pressure drop coefficient for a smooth slot.

the exit layer that turns from near the channel wall upstream of the slot entry and passes into the slot. Another feature is the large vortex on the upstream wall that is quite similar to that in Figure 2. The slot flow passes around the vortex creating a *vena contracta*. The general trend in Figure 7 is that reductions in the size of the recirculating zone are associated with smaller values of K. A variable f is defined as the fraction of the slot width filled by the vortex along a plane where the vortex has created the greatest restriction. One sees that at $V_S = 0.2$ m/s, $f = 0.85$ and $K = 400$. As V_S increases to 5.8 m/s ($V_N = 0.76$) both f and K decrease sharply, to 0.40 and 2.5 respectively. This corresponds to the diminishing regime noted in Figure 6. A further increase in V_S to 9.3 m/s ($V_N = 1.21$) leads to a relatively small decrease in f and K, to 0.31 and 2.0 (constant regime). The fact that f also shows a diminishing/constant relationship with V_N provides further evidence of the strong influence of f on K. One must note that while values of f follow expected trends, the precise dimensions of recirculation zones are poorly predicted by the k-ε method, and the estimates of f should be used with caution.

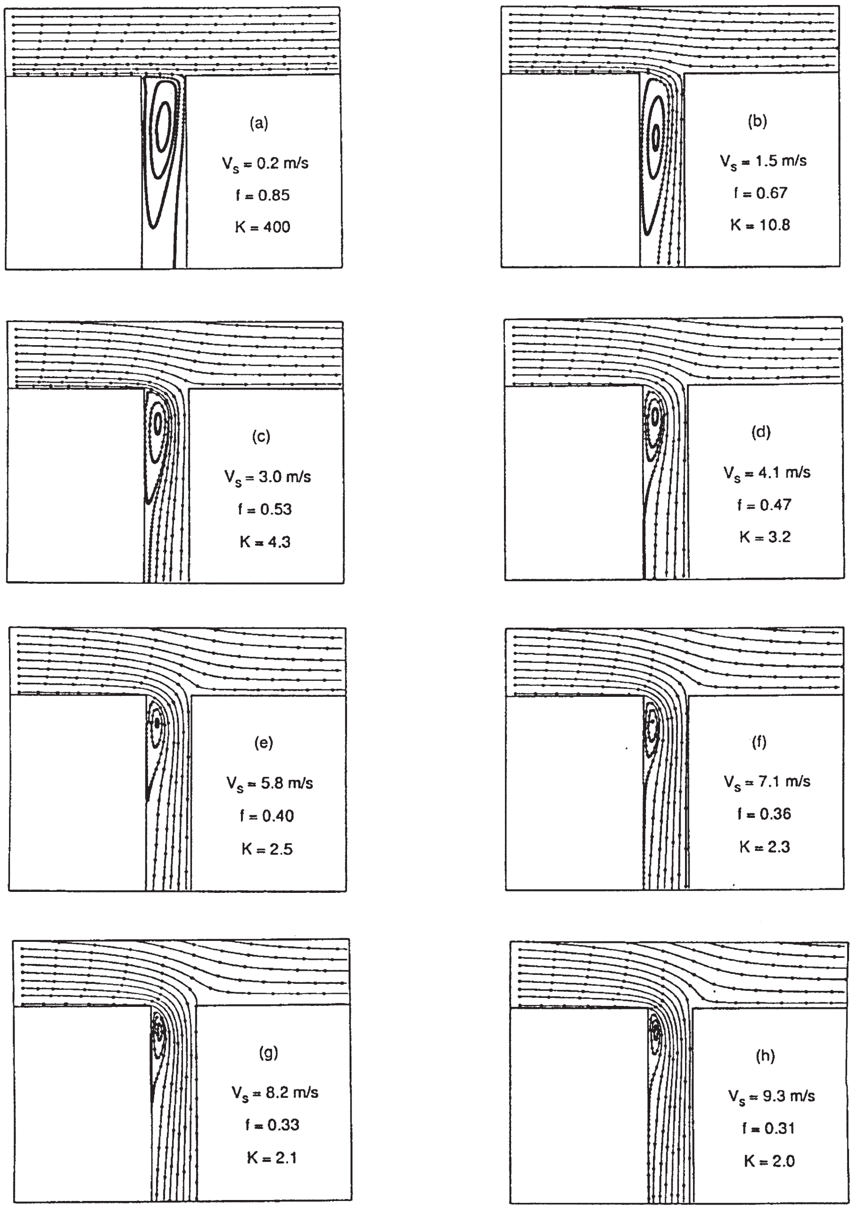

Figure 7 Flow patterns in a smooth slot ($V_U = 7.5$ m/s, $w = 0.5$ mm).

The recirculating zone in the slot is not the only factor that determines K. A more general technique is required to identify the flow structures that determine K, and this will become especially important for complex flow geometries where several recirculating zones may exist. Plots of turbulence intensity are proposed for this purpose, where turbulence intensity is defined as:

$$I = \frac{k}{\frac{1}{2}V_S^2} \tag{3}$$

Note that the lower-case k used here represents turbulent kinetic energy as opposed to the upper case K, which refers to the pressure drop coefficient. One cannot make a simple, quantitative connection between I and K. A strong correlation is to be expected, however, because turbulence eventually becomes energy loss (i.e., pressure loss).

To identify the flow structures that determine K one can compare plots of I for cases with high and low values of K. This is done in Figures 8

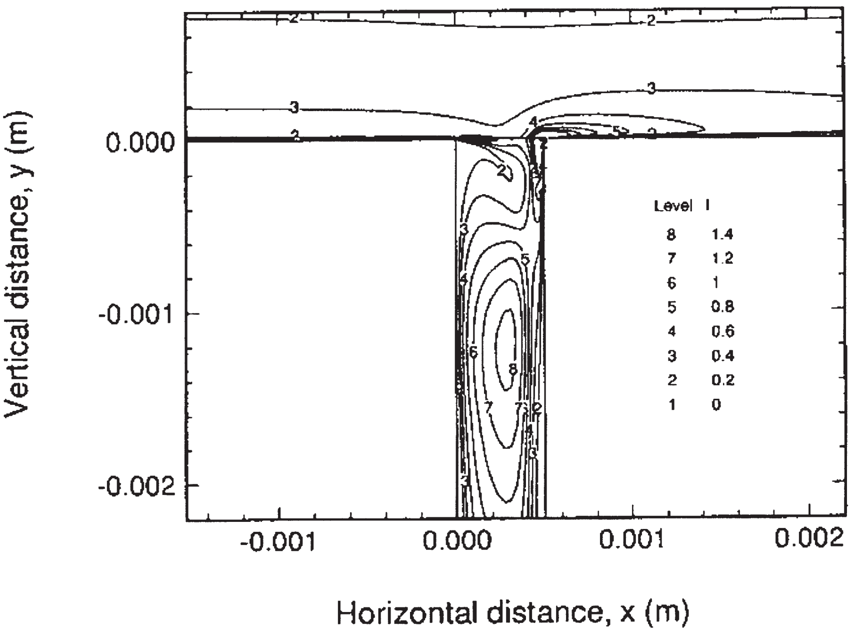

Figure 8 Turbulence intensity in a smooth slot ($V_S = 1.5$ m/s, $K = 10.7$).

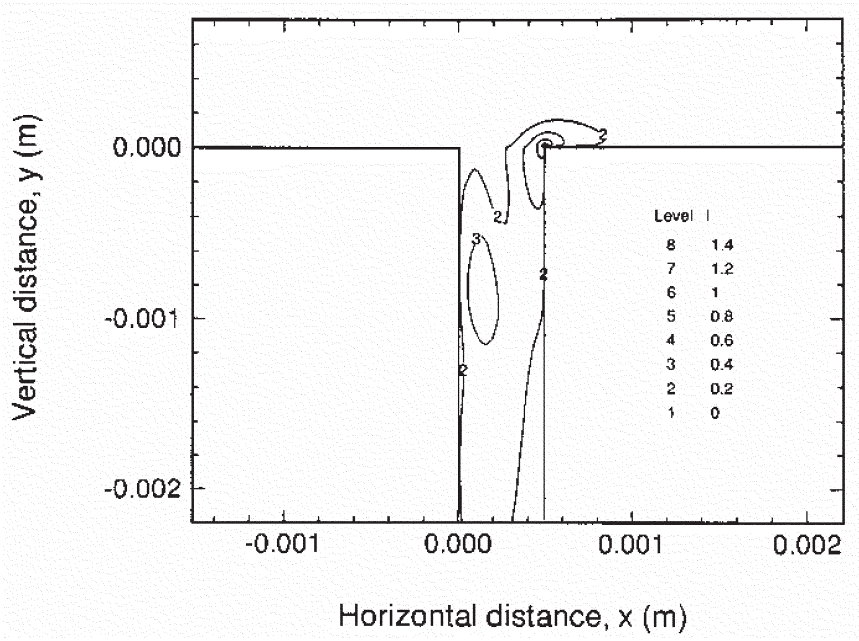

Figure 9 Turbulence intensity in a smooth slot ($V_S = 8.2$ m/s, $K = 2.1$).

($V_S = 1.5$ m/s, $K = 10.8$) and 9 ($V_S = 8.2$ m/s, $K = 2.1$). These figures confirm that K increases with I. For the high-K case, I is above 1.0 over much of the slot width at a plane just below the vortex. Maximum values are in excess of 1.4. For the low-K case, the maximum values of I are less than 0.6. The correlation of K and I supports the use of this method to identify the sources of K. The specific sources of K at low-V_S (Figure 8) would appear to be just below the vortex and on the downstream corner of the slot entry. The same sources exist at high-V_S (Figure 9), but the source on the downstream corner has become more significant.

While smooth slots are an appropriate starting point for this analysis, industrial pulp screens mostly use contour slots. Figure 10 shows the pressure drop characteristics for the step-step contour geometry generally used in this analysis ($w = 0.5$ mm, $w_C = 0.5$ mm, $d_C = 0.5$ mm). A significant reduction in pressure drop relative to smooth slots is apparent at high slot velocities. In such conditions, the reduction in hydraulic resistance (i.e., increase in capacity) would support the acceptance of contoured screen plates. At the more

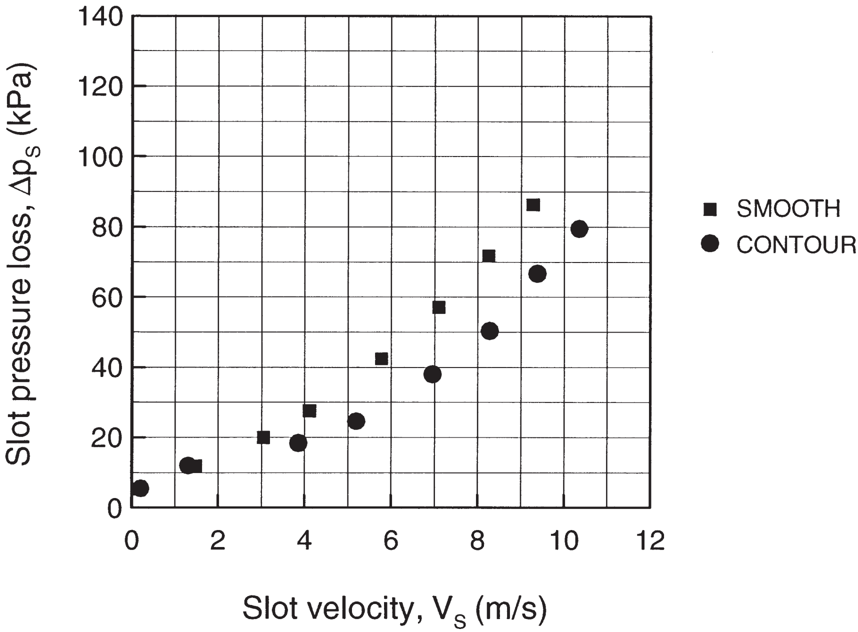

Figure 10 Pressure loss for smooth and contour slots ($V_U = 7.5$ m/s).

typical slot velocities below 2 m/s, however, the hydraulic resistance of the contour slot is about equal to that of the smooth slot.

The general relationship between K and V_N (Figure 11) is the same for the contour and smooth slots, which suggests that the underlying sources of pressure drop have remained fundamentally the same. A detailed examination of the flow patterns is useful to understand what the contour has done to reduce K at high V_N, while maintaining the form of the K-V_N relationship.

Figure 12 shows the changing flow patterns in the contour slot for increasing V_S. At $V_S = 0.2$ m/s, there are two large vortices present. One is set in the contour. The other vortex is in the slot and occupies 62% of the slot width. It is notable that the vortex is on the downstream side of the slot – not the upstream side, as was the case for the smooth slot. An increase in V_S to 1.3 m/s caused a substantial reduction in the size of the vortex in the contour, but relatively little reduction in the size of the vortex in the slot. The main decrease in f occurred when V_S was increased from 1.3 to 5.2 m/s. This corresponds to the region in Figure 11 where the line for the contour slot departs

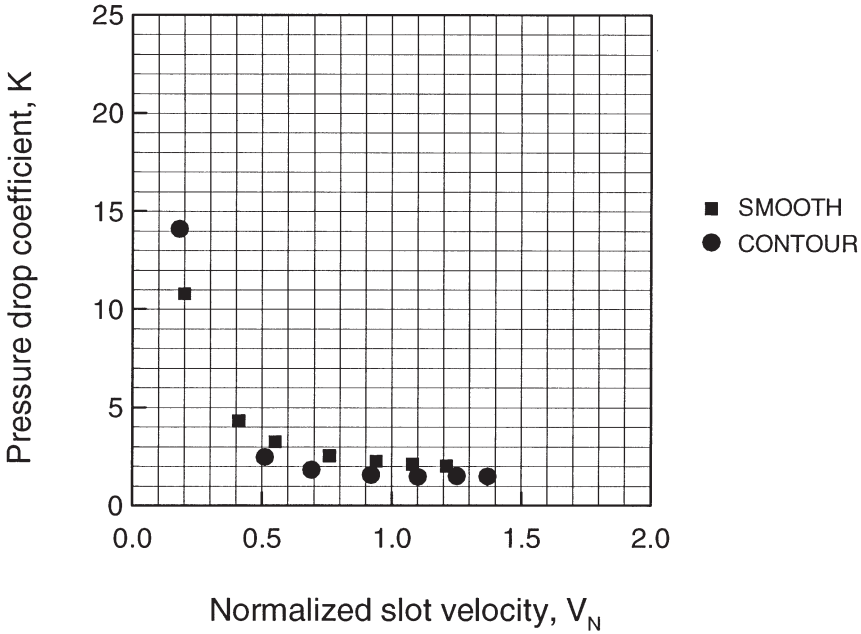

Figure 11 Pressure drop coefficients for smooth and contour slots.

from the line for the smooth slot. Further increases in V_S led to the complete elimination of a vortex within the slot. The fact that f was reduced to 0.00 in the contour slot, but only to 0.31 in the smooth slot would appear to underlie the contour slot's lower value of K at high V_S.

Sites of high I were previously associated with high energy losses and local sources of K. Figure 13 shows levels of I for a contour slot with a low slot velocity ($V_S = 1.3$, $K = 14.1$). Levels of I are generally over 0. 6, which is lower than the levels found for the smooth slot in Figure 8. The areas of high I extend over a larger area though, and there are significant areas where I is above 1.0. Thus it is not surprising that the overall values of K for the smooth and contoured slots are comparable at this slot velocity. At a higher slot velocity ($V_S = 8.3$, $K = 1.5$) levels of I were substantially reduced (Figure 14). For most of the contour and slot area, I is less than 0. 2. This is much lower than the levels of I found for a smooth slot at high V_S (Figure 9).

These findings further support the correlation between I and K. The usefulness of I comes in identifying the sources of K. At low V_S (Figure 13) the

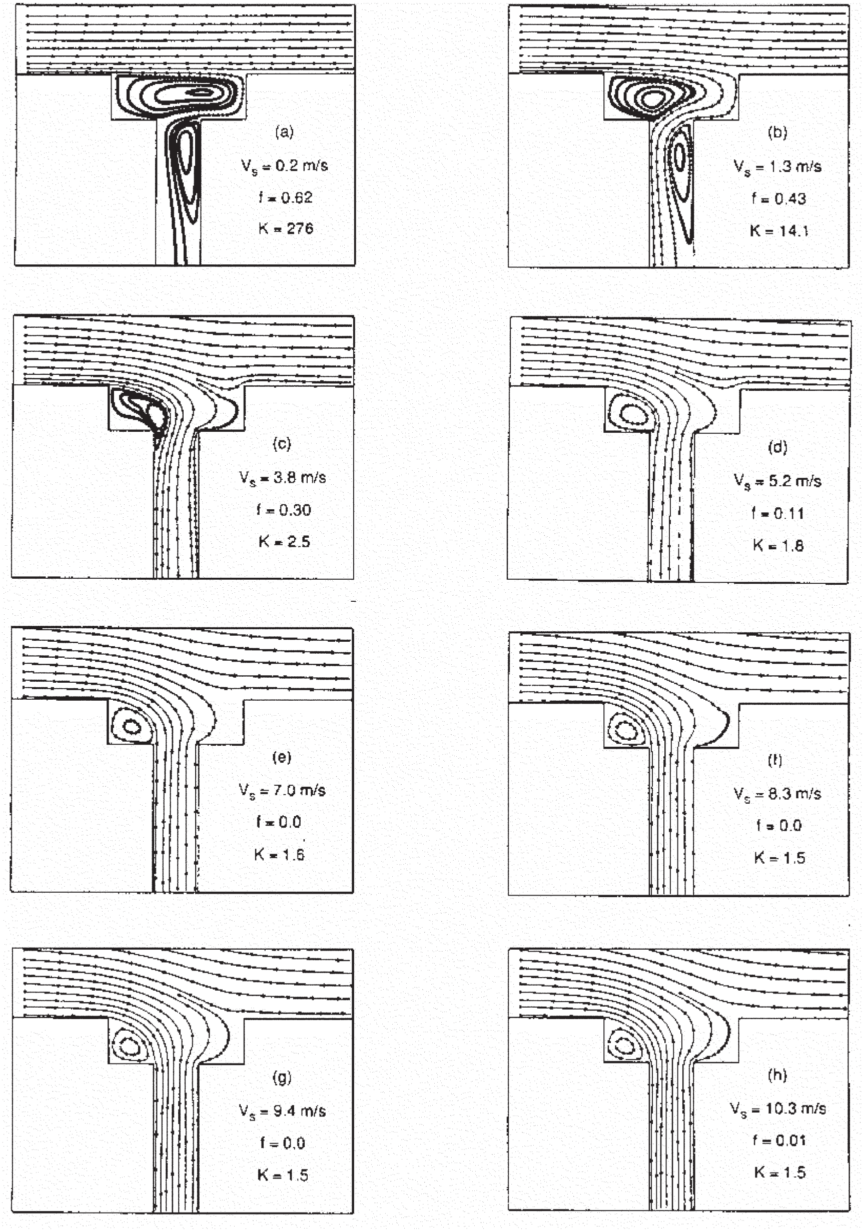

Figure 12 Flow patterns in a contour slot ($V_U = 7.5$ m/s, $w = 0.5$ mm).

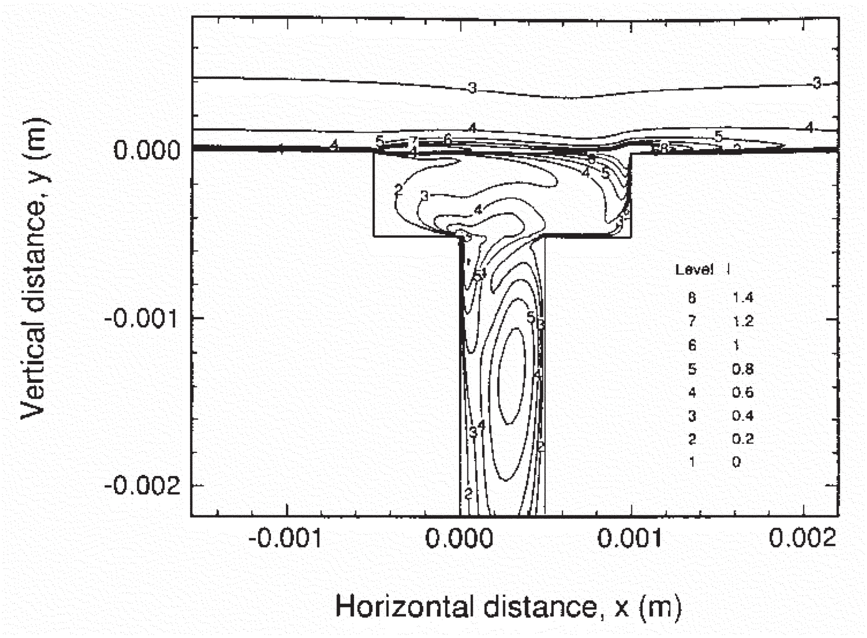

Figure 13 Turbulence intensity in a contour slot ($V_S = 1.3$ m/s, $K = 14.1$).

sources appear to be: 1) below the vortex in the slot, 2) on the upstream corner of the slot entry, and 3) on the downstream edge of the contour entry. For high V_S (Figure 14), the only significant source of K is on the downstream edge of the slot. This implies that reduced K at high V_S would come by altering the geometry on the downstream corner of the slot entry.

A range of slot geometries was analyzed to determine the optimum slot width/depth for the rectangular contour at $V_S = 3.7$ m/s and $V_U = 7.5$ m/s. The results are shown in Figure 15. They indicate that for $V_N = 0.\ 5$, minimum values of K occur at slot depths in the range of 0.25 to 0.50 mm and step-widths in the range of 0.5 to 1.5 mm. Very deep or very narrow contours lead to levels of hydraulic resistance that are equal to, and in some cases greater than those for a smooth slot. Note that Figure 15 considers the optimal contour dimensions for minimizing hydraulic resistance. These may not be the optimal contour dimensions for minimizing screen blockages or other important factors in screening.

This section has shown the benefits of CFD in both estimating pressure loss and providing a mechanistic explanation for the sources of the pressure

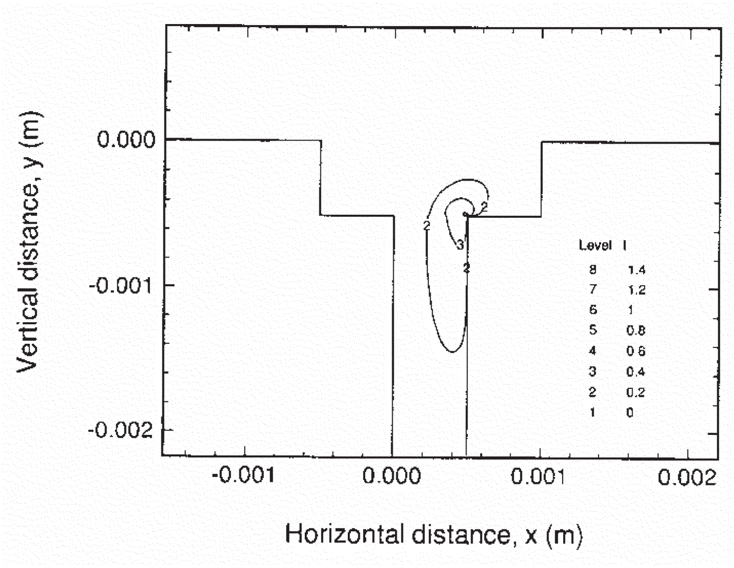

Figure 14 Turbulence intensity in a contour slot ($V_S = 8.3$ m/s, $K = 1.5$).

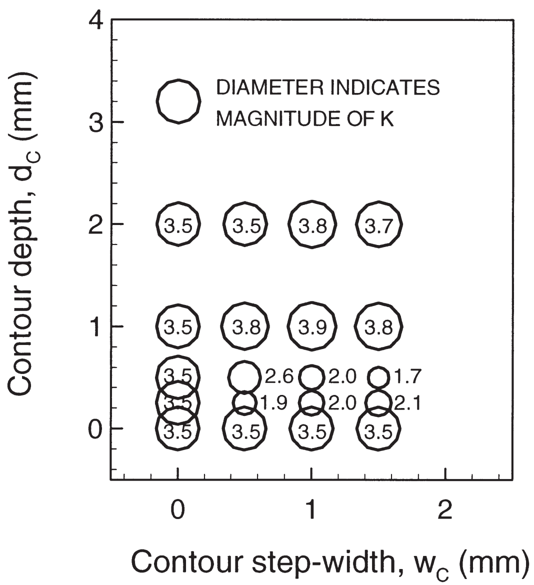

Figure 15 Sensitivity of K to contour depth and step width ($V_N = 0.5$).

loss. Furthermore, in cases where resistance is due to pulp accumulations, CFD can also be used to estimate the turbulence and shear levels available to break up the floc – or where local flow patterns might lead to an accumulation of fibres.

FLOW LOOP EXPERIMENTS

Experiments are required to validate the CFD solutions, and to assess the significance of factors that could not be included in the CFD work, such as the influence of fibre accumulations at the slot entry.

Experimental apparatus

Experimental studies were carried out using slotted coupons that fit into a screening channel that was, in turn, part of a flow loop. The flow channel and a typical coupon are shown in Figure 16 and details of the coupons, channel and flow loop are given in Gooding [39]. Most of the coupons had a single slot, though several had multiple slots. Some slots had feed-side screen

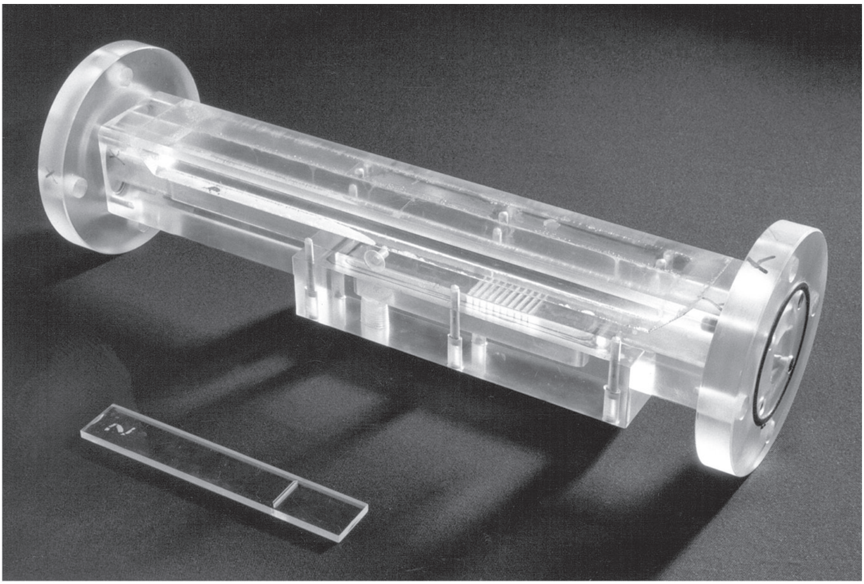

Figure 16 Flow channel and screen coupon with a single slot.

contours, with a step-step contour design being used in almost all cases. A slot width of 0.5 mm was generally used in this study though, as in the CFD studies, a limited number of tests were done with different slot widths. Coupons were made of transparent plastic to enhance visibility, which was especially valuable for tests where the size of fibre accumulations was measured. The thickness of each coupon was 5 mm, which is comparable to the thickness of industrial screen plates. Slot length was typically 15 mm versus the 65 mm length found in industry. This compromise was made to reduce the width of the channel and the flow volumes handled by the flow loop.

The screening channel was also made of transparent plastic and was comprised of two distinct chambers: a feed zone and an accept zone. Flow entered the feed zone from one side and exited through the other side. Turbulence induced by the contraction at the entry was intended to simulate the turbulence from the rotor in a pulp screen. The slotted coupon was set in the lower wall of the feed zone, and the distance from the entry to the slot was equal to half the distance between lugs on a rotor in an industrial screen. The distance from the surface of the coupon to the top of the feed channel was approximately equal to the distance between the screen plate and rotor core in an industrial pulp screen. The accept (lower) zone of the screening channel was a plenum that received the flow from the slot and passed it to a small outlet. The depth of the plenum was approximately equal to the distance between a screen plate and the outer casing of an industrial pulp screen. The three components of the screening channel (i.e., the feed zone, coupon and accept zone) fit together as a watertight assembly. The simple coupon design and ease of replacing coupons represented significant improvements over screening channels used in previous studies [11,12]. The screening channel also included sites for pressure transducers.

A flow loop was built to circulate water or pulp suspensions through the screening channel and it is shown in Figure 17. A centrifugal pump with a variable-frequency drive drew from a reservoir tank and delivered the flow to the feed pipe of the channel. The discharge flow from the feed zone of the channel then passed through a pipe and a control valve to an atmospheric discharge at the reservoir. By adjusting the control valve and variable-speed pump drive, one could provide the desired pressure and flow rate in the screening channel. A separate path was taken for the accept flow that passed through the slot in the channel. It left the accept plenum and passed through a control valve to an atmospheric discharge at the accept tank. A submersible pump returned this flow to the main reservoir to permit continuous operation of the loop. Magnetic flowmeters were installed on the feed and accept lines to provide measurements of the volumetric flows. Average

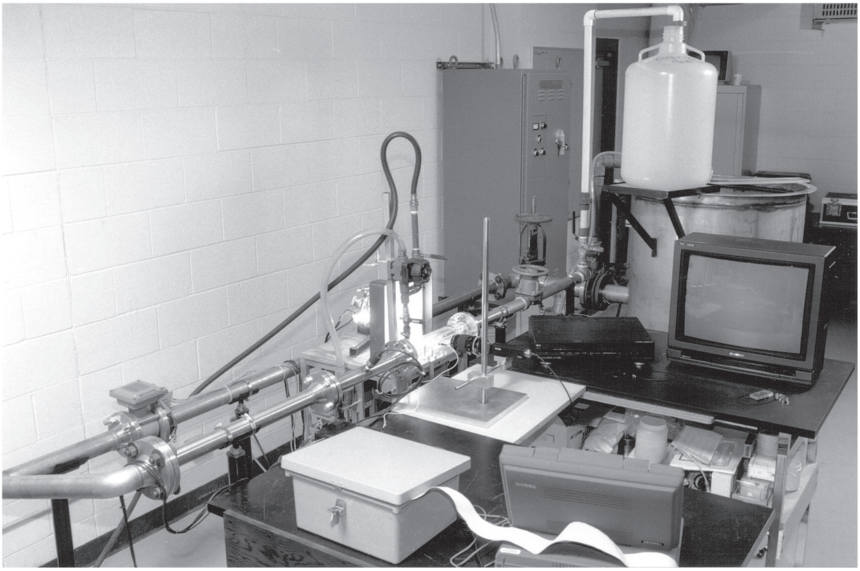

Figure 17 Flow loop for flow channel tests.

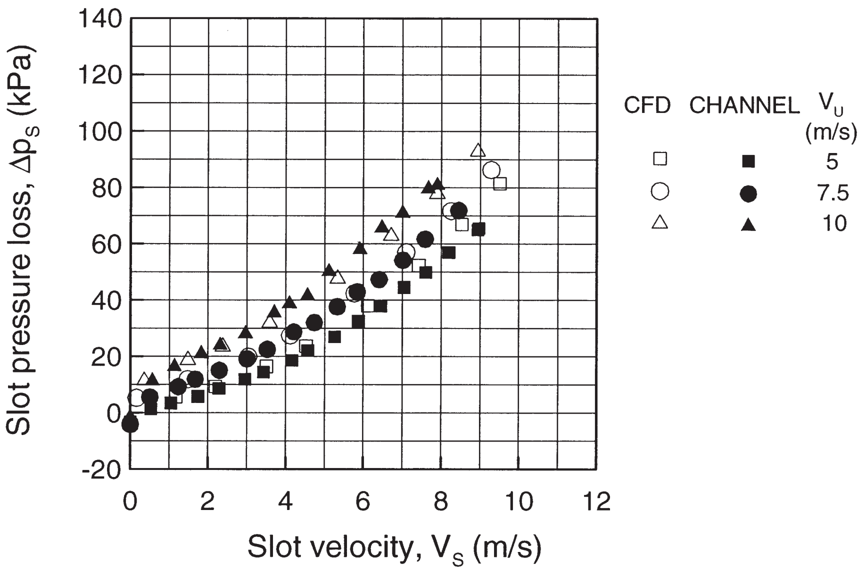

Figure 18 Pressure loss for a smooth slot.

upstream velocity in the channel and average slot velocity for the accept flow were obtained by dividing the volumetric flows by the cross-sectional area of the channel duct and slot respectively. Pressure drop was measured by pressure sensors in the feed channel and in the pipe from the accept plenum. In each case, the measuring points were set sufficiently far from flow disturbances so that one could assume the cross-channel pressure gradients were small and pressures measured at the wall would be representative of the pressure in the bulk flow. A computer-based data acquisition system displayed values of flow and pressure. The data acquisition system also recorded precise measurements of pressure and velocity, each based on an average of at least 50 sets of pressure and velocity values taken over a 5-second period.

Results: water flows

Pressure loss was assessed for a range of slot velocities and three upstream velocities through a smooth slot, as shown in Figure 18. The figure shows that experimental results compare closely (within 5%) with CFD predictions for $V_U = 7.5$ m/s. As with the CFD results, the one-dimensional energy equation was applied to the flow through the slot to determine the pressure loss of the aperture distinct from other influences that would affect the measured pressure drop. In this way, compensation could be made for elevation effects, changes in velocity, pressure losses attributable to the displacement of the pressure sensors from the slot, and kinetic energy correction factors that account for the velocity gradients, as discussed in Gooding [39].

Normalized values of pressure drop and slot velocity are given in Figure 19. The curves feature a descending regime for V_N less than 0.5, and a constant regime for higher values of V_N. Normalization did not cause the effect of V_U to disappear completely, e.g., values of K for $V_U = 5$ m/s are slightly lower than for the other values of V_U. However, the good agreement with CFD results seen in Figure 18 is also found here. For example, at $V_N = 1$, K was estimated to be 2.1 from experimental results ($V_U = 5$ m/s) versus a value of 2.2 from CFD.

The effect of slot width was assessed for smooth slots and the results are shown in Table 2. At a low slot velocity, wider slots led to increased hydraulic resistance. At a high slot velocity, K was less sensitive to w. Both of these effects are consistent with the CFD findings, but as with Figures 18 and 19, some discrepancies exist and there are a number of possible causes: (1) differences in slot depth could affect the size of the vortex in the slot; (2) the side walls of the screening channel would introduce significant three-dimensional effects into a flow that is intended to be two-dimensional; (3) turbulence intensity in the channel may be higher than the 0.3% value used for the CFD

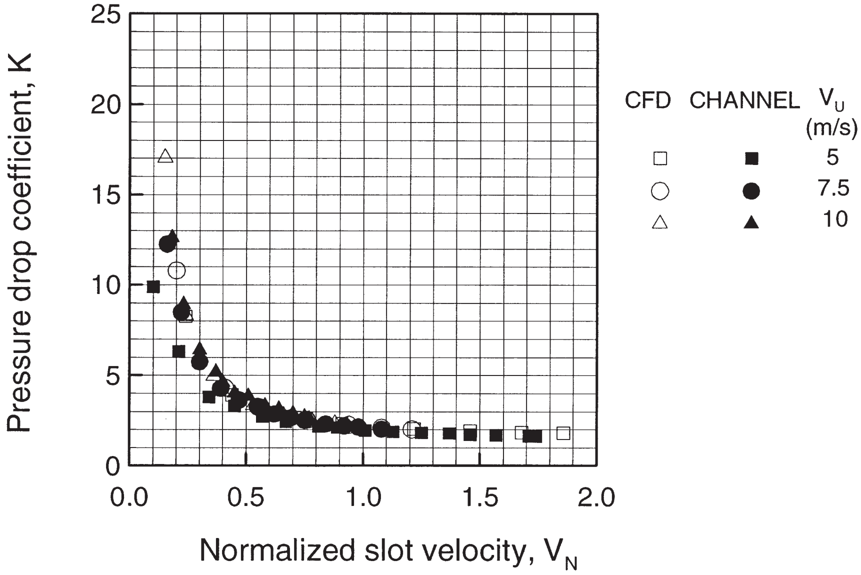

Figure 19 Pressure drop coefficient for a smooth slot.

Table 2 Effect of slot width on *K* for flow channel (FC) and CFD tests for smooth slots.

V_N	*K*					
	0.25 mm[1]		0.5 mm[1]		1.0 mm[1]	
	FC	CFD	FC	CFD	FC	CFD
0.2	8.6	9.7	9.8	10.8	13.0	12.0
0.9	3.0	2.4	2.2	2.3	2.7	2.2

[1]Post-facto measurement of slot widths revealed actual FC slot widths to be: 0.30, 0.50 and 0.86 mm.

inlet conditions; (4) imperfections in the slots cut in flow channel coupons could cause differences with the CFD results. In particular, the CFD analysis was based on a sharp-edged slot where the radius of curvature (*r*) of the corners at the slot entry is 0. In the flow channel study, the slot corners were generally sharp, but for certain coupons, imperfections produced a radius of curvature, r, in the order of 0.05 mm, i.e., a value of $r/w = 0.1$. This is thought to be significant since increasing r/w from 0 to 0.1 causes K to decrease by a factor of 4.2 for flow entering a circular pipe [41].

Values of Δp_S and K for step-step contour slots are shown in Figures 20 and 21. The data are for a 0.5 mm-wide slot that has a step-step contour with 0.5 mm depth and 1.0 mm step-width. The $\Delta p_S - V_S$ curves for smooth and contour slots (Figure 20) have a generally similar shape except for the presence of a plateau region for the contour slot in the range of $2 < V_S < 4$ m/s. Through this range, Δp remains relatively constant despite the fact that slot velocity doubles. The CFD results in Figure 10 also showed a plateau region, but it was less pronounced, perhaps because the step-width was 0.5 mm instead of the 1 mm for the flow channel. As shown in Figure 12, there is strong evidence that the plateau region results from the decreasing size of vortices in the contour and slot.

The step-step contour represents only one class of contour designs. Another, perhaps more widely used, contour is the step-slope design

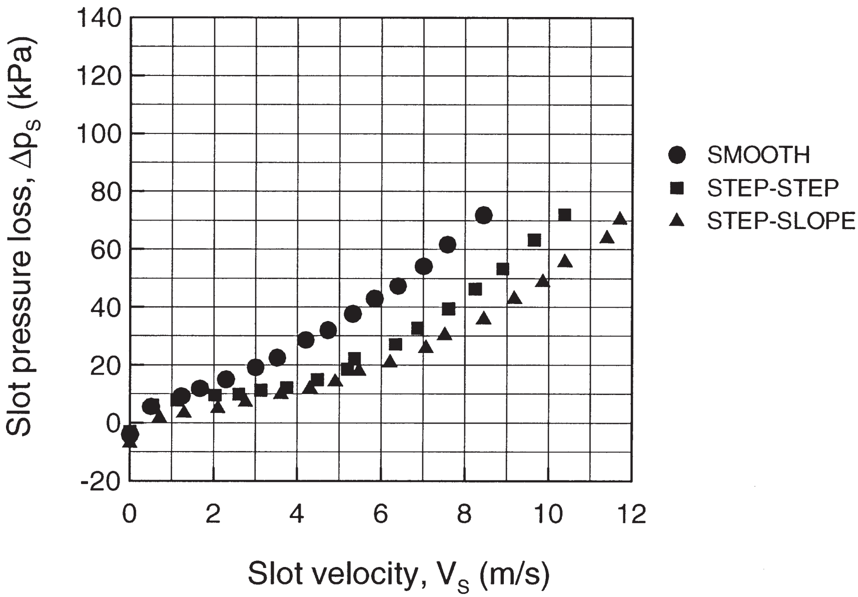

Figure 20 Pressure loss for smooth and two types of contour slots ($V_U = 7.5$ m/s).

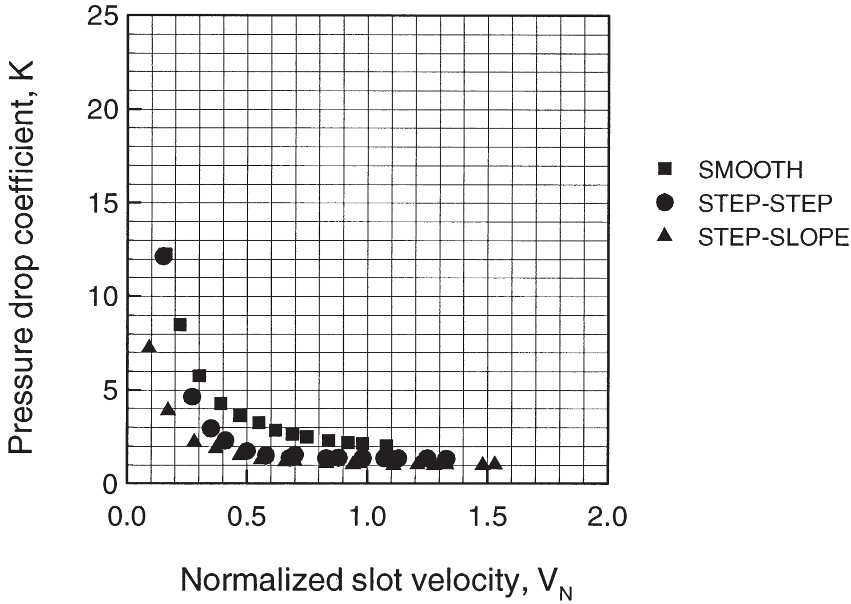

Figure 21 Pressure drop coefficient for smooth and two types of contour slot.

(commercially known as the *Profile*^{TM} contour) shown in Figure 22. The hydraulic resistance of this contour is also shown in Figures 20 and 21. Figure 20 demonstrates the low values of Δp_S that can be obtained with the step-slope contour, especially at high velocities. Significant reductions in resistance were also noted at lower, more industrially significant, slot velocities. Figure 21 shows that at $V_N = 0.2$ ($V_S = 1.5$ m/s) the step-slope contour reduces K by 75% relative to the smooth slot, and 60% relative to the step-step contour.

The sensitivity of K to contour dimensions was examined experimentally. Figure 23 shows that for $V_N = 0.\ 5$, the minimum value of K (= 1.9) was for a contour with $d_C = 0.5$ mm and $w_C = 1.0$ mm, i.e., the contour geometry used for Figures 20 and 21. This value of K was much less than that for a smooth slot, which is shown in Figure 23 where $d_C = 0$ or $w_C = 0$. It was also less than the values of K for deeper slots, which in several cases were greater than that for the smooth slot. These findings are in good agreement with the CFD findings, both in terms of the values of K and in the optimal contour dimensions.

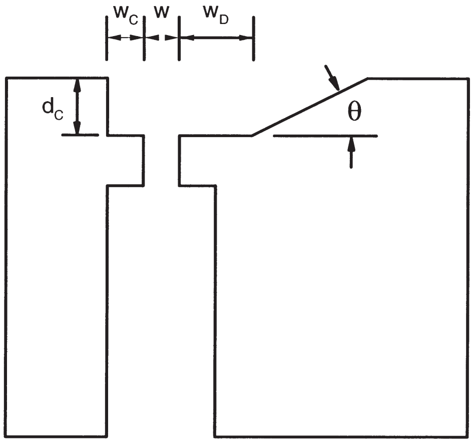

Figure 22 Step-slope (*Profile*^{TM}) contour. Drawing is not to scale.

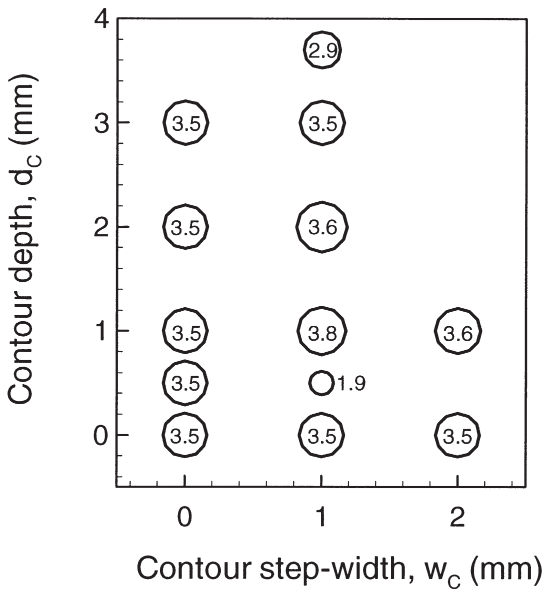

Figure 23 Sensitivity of K to contour dimensions ($V_N = 0.5$).

Multiple slots are of high interest since they represent the configuration in a commercial screen. The hydraulic resistance of slots in series was examined in flow channel tests. The slots had a step-step contour with $d_C = 1$ mm, $w_C = 1$ mm, and an inter-slot spacing of 5 mm. Combinations of one, two, three and four slots were examined, and the results are shown in Figure 24. There was no appreciable effect of multiple slots on hydraulic resistance for flow velocities up to 4 m/s, which would be expected to embrace the typical slot velocities found in industrial pulp screens.

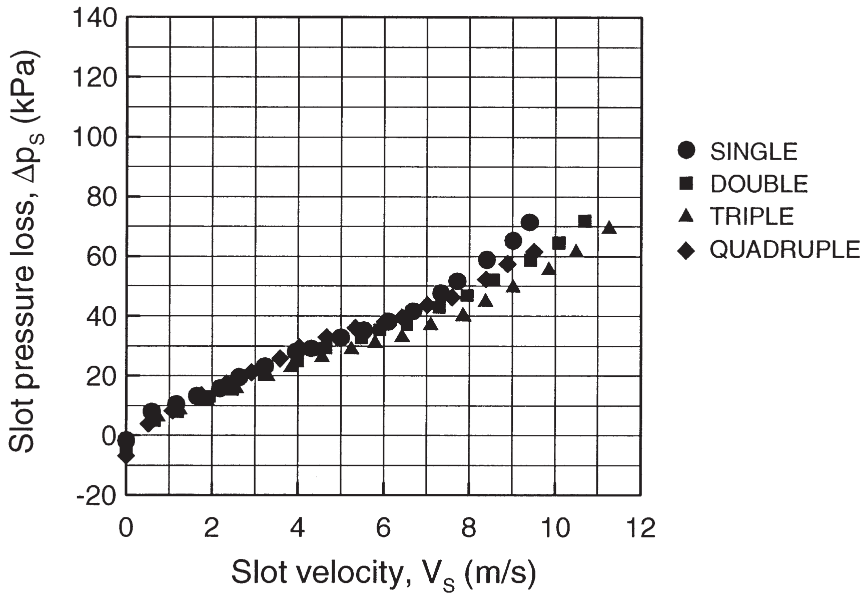

Figure 24 Pressure loss for multiple contour slots ($V_U = 7.5$ m/s).

Results: fibre accumulations

A study of flow resistance in pulp screens must consider the effect of fibres in the flow, and the potential for fibres to accumulate in the screen plate apertures. This was studied by passing a dilute fibre suspension through the flow channel and monitoring the pressure loss as fibres accumulated within the screen slot. A 1 mm wide smooth slot was used for these tests. This width is larger than what is typical industrially, but it provided greater precision in

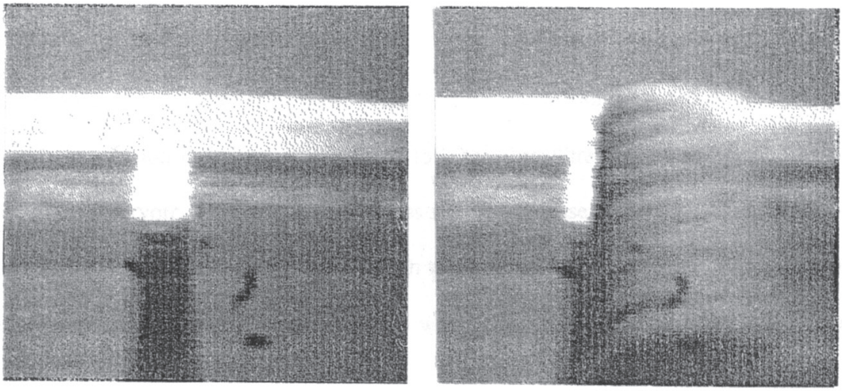

Figure 25 Typical images from fibre accumulation study showing an open slot (left) and partially-filled slot (right).

measuring fibre accumulations. A suspension with a concentration of 158 000 fibres/liter (approx. 0.04% consistency) was used, which was low enough to prevent fibre interaction upstream of the slot, but high enough to cause an appreciable accumulation of fibre over the one minute test period. Trends of pressure and flow were recorded to provide at least 250 measurements over the test period. The size of fibre accumulations in the slot entry was measured using a borescope and video camera (20 frames/second), and some sampled images are given in Figure 25. The size of the accumulation was defined as the percentage of the slot that was filled. Analysis of the video images was made manually, frame-by-frame, by overlaying a scale on the video monitor. A quantity f_{VIS} was defined as the fraction of the slot width (w) that was filled with fibres, and the subscript refers to the fact it was obtained through visual observations. The slot was purged before the start of a fibre accumulation event. During the test, the control valve was not adjusted to maintain either a constant slot velocity or a constant pressure drop across the slot. What remained constant was the overall pressure drop between the channel and the discharge of the accept flow line.

The results of a typical trial are shown in Figure 26. It shows that as the fibre build-up increases, the flow through the slot drops and hydraulic resistance increases. Both effects are initially strong, but diminish over time. The same trends are reflected in the measurements of f_{VIS} given in Figure 27. The associated video images show that fibres initially accumulate rapidly on the downstream edge of the slot, but then a steady state is approached

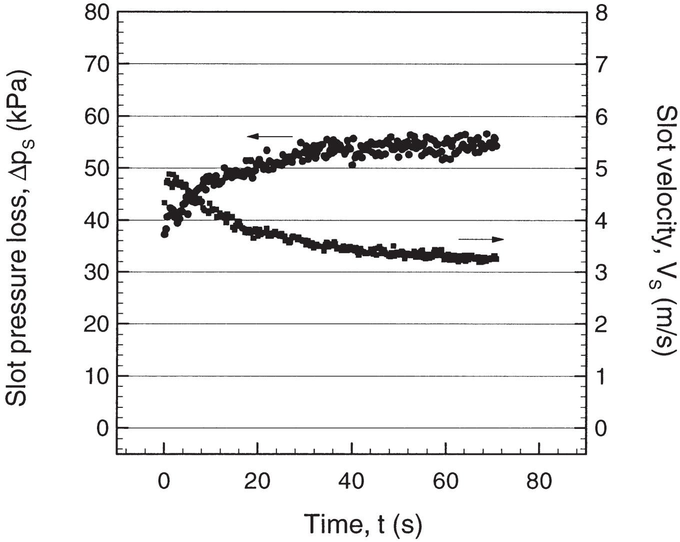

Figure 26 Effect of fibre accumulation on pressure loss and slot velocity.

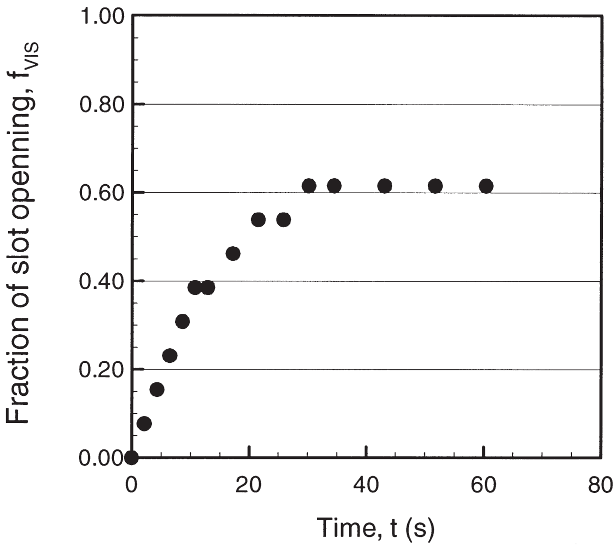

Figure 27 Rate of fibre accumulation from video images: V_S (initial) = 5 m/s.

where the deposition of fibres is balanced by fibre shedding. One problem with the visual measurements of the fibre accumulations is that f_{VIS} does not account for porosity within the fibre accumulation. One would expect some porosity to exist, at least on the outer layer of the fibre accumulation. An alternate variable, f_K, is thus proposed which is based on the measurements of K and follows from the assumption that the changes in K simply reflect narrowing of the slot. A new set of variables is thus defined: w', V_S' and K'. These are analogous to w, V_S and K, but are based on the open area of slot. Thus:

$$w' = (1 - f_K)w \tag{4}$$

$$V'_S = \frac{V_S}{(1 - f_K)} \tag{5}$$

$$K' = \frac{\Delta p_S}{\frac{1}{2}\rho(V'_S)^2} = \frac{\Delta p_S}{\frac{1}{2}\rho V_S^2}(1 - f_K)^2 \tag{6}$$

$$= K(1 - f_K)^2$$

At the start of a test, the slot is clear ($f_K = 0$) and $K' = K$. Figure 26 shows that as the fibre accumulation grows, Δp_S increases and V_S decreases. Following on its definition in equation 1, the value of K will also increase. However, for the calculation of f_K one assumes that the value of K' remains constant and the change in K simply reflects the decrease in slot width and associated increase in V_S. Equation 6 can be rewritten to express f_K explicitly:

$$f_K = 1 - \left[\frac{K'}{K}\right]^{\frac{1}{2}} \tag{7}$$

One can determine the value of K' from the value of K at the start of the test. Thus changes in K give a direct measurement of f_K.

The results of the fibre accumulation tests are summarized in Table 3 for a range of V_S. In the first test, for example, K rises from 16 to 22 during the one minute test while V_S drops from 0.9 to 0.7 m/s. Video measurements show that 15% of the slot width was filled with fibre ($f_{VIS} = 0.15$). Following on equations 4 to 7, one could also explain the rise in K by saying that 15% of the slot was filled ($f_K = 0.15$) and the velocity within the narrowed slot (V'_S) was 0.82 m/s at the end of the trial. Table 3 shows that a higher initial velocity led to a higher percentage of the slot being filled (assessed either by f_{VIS} and f_K).

Table 3 The effect of initial slot velocity on K, f_{VIS} and f_K.

V_S (*initial*)	K′ (*K initial*)	V_S (*final*)	K (*final*)	K'/K	f_{VIS}	f_K
0.9	16	0.7	22	1.4	0.15	0.15
1.9	6.5	1.8	8.6	1.3	0.54	0.13
2.9	4.3	2.6	9.8	2.3	0.54	0.35
3.9	3.8	2.8	10.8	2.8	0.63	0.41
4.9	3.3	3.3	10.3	3.1	0.62	0.43
4.8	3.5	3.2	10.3	2.9	0.62	0.42
5.8	3.0	3.7	9.4	3.1	0.54	0.44
6.6	2.7	3.9	8.9	3.3	0.54	0.45
7.6	2.4	4.2	8.0	3.3	0.56	0.45

At an initial slot velocity of 5 m/s, the slot becomes about half-filled with fibres and the value of K more than doubles in the one minute test period. One should not, however, associate the size of fibre blockages and the increase in K with particular slot velocities in a general sense. The deposition of fibre flocs within a pulp screen at realistic pulp consistencies might well be governed by different mechanisms.

While the values of f_{VIS} and f_K follow similar trends, they differ in values, especially in the range of V_S (initial) between 1.9 and 3.9 m/s. The value of f_{VIS} would be expected to overestimate slot blockages because it does not account for changes in the porosity in the fibre accumulation. Porosity would be expected to decrease with increasing slot velocity (i.e., as the pressure from the flow compacts the fibre accumulation). Indeed the agreement between f_K and f_{VIS} improves at an initial slot velocity greater than 3. 9 m/s. Conversely, values of f_K would be expected to underestimate the size of the slot blockage. This is because the initial value of K' would not be expected to remain constant as the accumulation grows, but would be sensitive to the reduction in slot velocity, the narrowing of the slot, and the change in flow pattern caused by the fibre accumulation. The actual slot blockage is likely to be some intermediate value between f_{VIS} and f_K.

This section has demonstrated the good agreement between flow channel tests and CFD findings. This embraced an understanding of the effect of V_S and V_U on K for water flows with both smooth and contour slots, and for contours with different dimensions. Flow channel tests have extended this knowledge with studies of fibre accumulations. An accumulation for fibres that appeared to fill half of the slot led to K increasing by a factor between 2 and 3. Thus the resistance due to simple water flow, and the resistance due to fibre accumulations are both significant for these particular conditions.

PILOT PLANT TRIALS

Trials with an industrial pulp screen were conducted to extend the more fundamental insights developed in the CFD and flow channel studies. The work was conducted in a pilot plant setting so that the screen could be operated over a wide range of variables, under controlled conditions, and with a high degree of instrumentation. While these tests were done in a pilot plant, they were conducted under conditions very similar to those in pulp mills.

Experimental

The pulp screen used for these tests was a Hooper PSV 2100 screen and it is shown in Figure 28. The rotor in the Hooper screen uses hydrofoils to induce

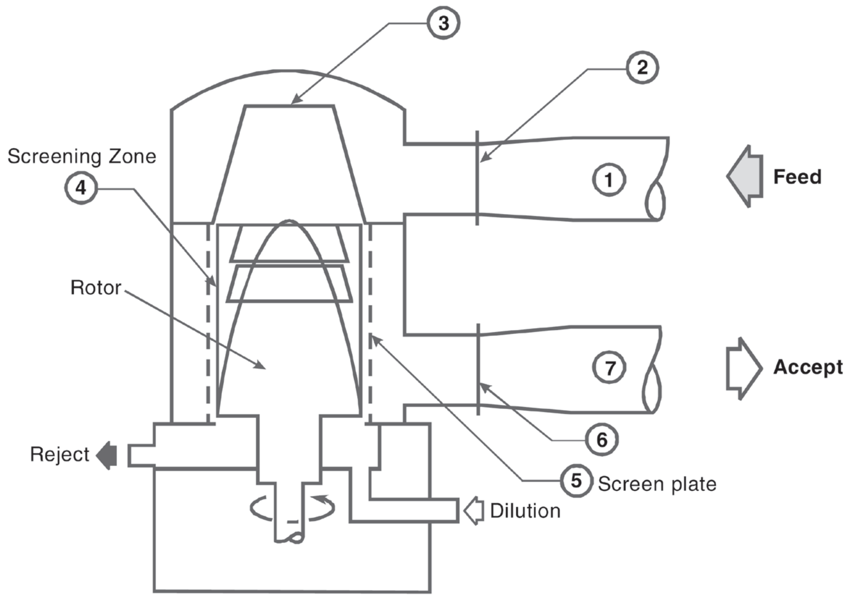

Figure 28 Schematic of Hooper PSV 2100 screen. Numbers identify reference locations for pressure loss assessment.

Figure 29 Rotor for Hooper PSV 2100 pulp screen.

a high tangential velocity, and to produce pressure pulsations which back-flush the screen plate apertures. A photograph of the Hooper rotor is given in Figure 29. Rotor speed is typically in the range of 750–1450 rev/min, which yields tip speeds of 11.7 to 21.8 m/s. Different tip designs may be installed on the Hooper screen, and in this study, 54 mm-wide tips were set at a distance of about 2.5 mm from the screen plate. A baffle assembly at the top of the rotor is intended to spread the feed flow along the surface of the screen plate. The screen plate used in this study had vertical, 65 mm long, 0.53 mm-wide slots and a step-step contour ($w_C = 0.89$, $d_C = 0.92$). The slot-to-slot spacing was 4.23 mm. The screen plate was made of stainless steel, and was electro-deburred and chrome-plated after being formed. The plating process does not deposit material uniformly, and the corners within the slot were rounded somewhat, unlike the relatively sharp corners in the plastic coupons used for the flow channel tests.

Typical accept and reject flow rates for the Hooper PSV 2100 screen are 2000 and 500 litres/min respectively. It is useful to estimate the local velocities

Table 4 Calculated local velocities within a Hooper PSV 2100 Pulp Screen for typical operating conditions. No reject flow was used in the present tests.

Location	*Flow rate* (l/min)	*Area* (m^2)	*Velocity* (m/s)
Feed line	2500	0.0182	2.3
Cone entry	2500	0.0137	3.0
Screen plate slots	2000	0.0295	1.1
Accept Line	2000	0.0182	1.8
Reject Line	500	0.0046	1.8

at critical points in the screen from the flow rates and the local cross-sectional areas, and these are given in Table 4. Note that the slot velocity given in Table 4 is based on the assumption that the flow is steady and is spread equally amongst each of the 860 slots in the plate. This simplification neglects the flow transients that arise from the pressure pulsations, and the variations that may exist from one part of the screen plate to another. The velocity parallel to the screen plate is not included in Table 4, but it is assumed to be equal to the tangential velocity induced by the rotor, as discussed above. The axial component of velocity caused by the bulk flow through the annular area between the rotor core and screen cylinder is relatively small. If one considers the axial flow at the mid-point along the axis of the screen, the flow is roughly 1500 l/min and the annular area is about 0.030 m^2. This yields an axial component of velocity equal to 0.8 m/s, which is about an order-of-magnitude less than the tangential component of velocity induced by the rotor. The magnitude of a vector sum of the axial component and the tangential component differs by less than 1% from the magnitude of the tangential component alone.

The pulp screening pilot plant used for these tests had many of the same features as the flow channel flow loop, but on a much larger scale. Details of the pilot plant are given by Gooding [39]. The loop had an 11 000 liter stock tank where the water or pulp suspension was prepared. An open-impeller, centrifugal pump pumped the fluid through a control valve and magnetic flow meter to the screen inlet. The accept and reject flows from the screen then passed back to the stock tank after going through flow meters and control valves. Chemi-thermo-mechanical pulp was reslushed in the stock tank for tests with pulp. Pulp consistency was adjusted to a value of 1.5%, and the mixing action was continued until the fibres were fully dispersed. The starting temperature for a trial was typically adjusted to about 40°C.

Approach

The screen plate is assumed to be the principal source of flow resistance in the pulp screen, but it is not the only source. The approach followed here was to measure the overall pressure differential, assess the resistances of the individual components in the Hooper screen and determine the resistance of the screen apertures by differences. The analysis of the pressure screen is based on a control volume drawn around the pulp screen body, through entry and exit planes at Locations 1 and 7 respectively (Figure 28). Application of the energy equation yields:

$$p_1 + \alpha_1\left(\tfrac{1}{2}\rho V_1^2\right) + \rho g Z_1 + R = p_7 + \alpha_7\left(\tfrac{1}{2}\rho V_7^2\right) + \rho g Z_7 + \Delta p_T \tag{8}$$

where p_I, V_I and Z_I represent the pressure, velocity and elevation at any location "*i*", and α_1 is a velocity correction term that accounts for the non-uniform velocity profile in pipe flows [41], R is the pumping pressure created by the rotor, and Δp_T is the total pressure loss resulting from the sum of the flow resistances in the screen. The total pressure loss can be resolved into a series of pressure losses that are contributed by the various components of the screen, which can be appreciated by tracing the flow through the screen. The flow enters the control volume at Location 1 where the feed pressure is measured. After the flow passes through the feed flange (Location 2), it goes into the entry zone, through a cone-shaped rock trap (Location 3) and to the entrance of the screening zone between the rotor and screen plate. The flow is then subjected to the pumping action by the rotor. As a first approximation, the pumping pressure (R) is assumed to be independent of the feed flow rate. The screening zone is also where the feed flow is divided into an accept and reject flow. This analysis will only consider the accept flow path, since it is the flow that defines screen capacity. Equation 8 only applies to the particular case studied here where there was no reject or dilution flow. The same approach could, however, be easily adapted to include the effect of these additional flows [32] and thus provide a complete hydraulic model of the pulp screen. The next step is for flow to pass through the screen plate (Location 5). The pressure loss associated with passage through the screen (Δp_S) is the focus of this thesis. To complete the model of the feed-accept flow, the flow goes through the accept flange of the pulp screen (Location 6) and then to the plane where the accept pressure is measured (Location 7).

The pressure drop commonly measured in industry is the difference between the feed pressure (Location 1) and accept pressure (Location 7), which is defined here as the "industrial pressure drop", Δp_I:

$$\Delta p_I = p_1 - p_7 \tag{9}$$

The total pressure loss can be expressed as the sum of the pressure loss due to the screen and the sum of the various resistances through the screen housing, Δp_H:

$$\Delta p_T = \Delta p_S + \Delta p_H \tag{10}$$

One can assume $\alpha_1 = \alpha_7 = 1.05$ based on the assumption of fully-developed flow (41). Thus Equation 8 can be rewritten as:

$$\Delta p_S = \Delta p_I + 1.05\left[\tfrac{1}{2}\rho(V_2^2 - V_8^2)\right] + \rho g\,[Z_2 - Z_8] + R - \Delta p_H \tag{11}$$

To determine Δp_H for the industrial screen, Δp_I was measured for an empty screen housing, and then with progressively more of the screen internals added back in. With the screen plate and rotor removed $\Delta p_S = R = 0$. The dynamic term in equation 11 was determined from the flow through the pulp screen and the cross-sectional areas at Locations 1 and 7. The elevation term in Equation 11 and any offsets in the measurement system were determined before the start of the trial (i.e., by measuring Δp_I with the accept velocity $(V_A) = 0$, and consequently $V_1 = V_7 = \Delta p_H = 0$). For convenience, these various terms were collected as a quantity, H:

$$H = -\alpha\left[\tfrac{1}{2}\rho(V_1^2 - V_7^2)\right] - \rho g[Z_1 - Z_7] + \Delta p_H \tag{12}$$

and the relationship of $H = f(V_A)$ was used for all subsequent measurements. Equation 11 could then be further simplified to:

$$\Delta p_S - R = \Delta p_I - H = \Delta p_R \tag{13}$$

where Δp_R has been defined as the "apparent pressure loss". Thus measurements of Δp_I and a knowledge of H could be used to determine the Δp_R. In the plots of Δp_R versus V_S presented below, R is assumed to be independent of V_S and can be measured by the y-intercept of Δp_R (i.e., where $V_S = \Delta p_S = 0$). Accordingly, Δp_S can be assessed from these figures as simply Δp_R plus the constant value of R.

RESULTS

The empty screen housing produced a small, but significant, amount of flow resistance, as shown in Figure 30. At an accept velocity of 2 m/s the measured Δp_I was 2.0 kPa. The entry cone (rock trap) was added for the next test, and

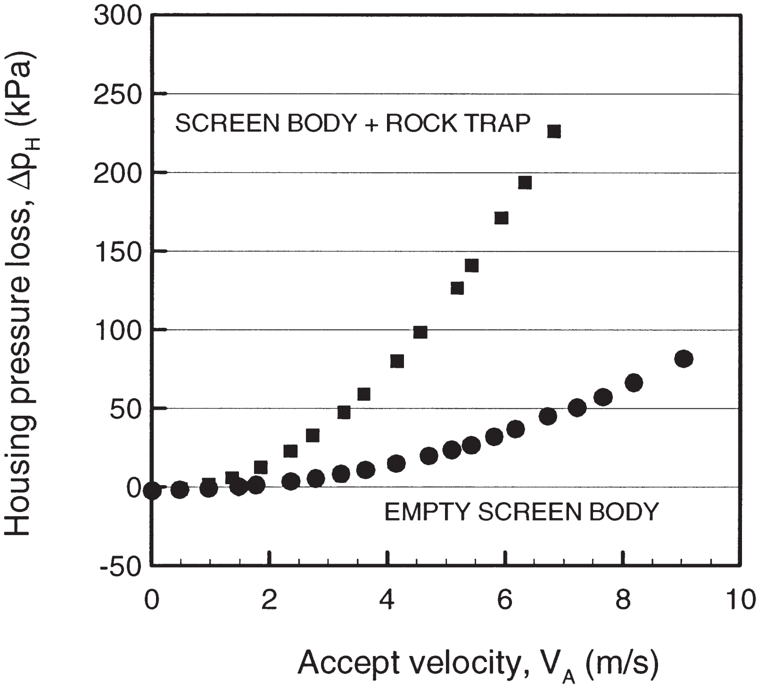

Figure 30 Pressure loss for screen body.

the values for Δp_H were surprisingly large. The high resistance of the entry cone is believed to reflect a design flaw in the particular screen used in this study and is not indicative of Hooper screens (or pressure screens) in general. The pressure loss data for the screen body and rock trap were expressed as a polynomial and used to define Δp_H in equation 12.

Tests with the pulp screen in its normal configuration, with the screen cylinder and rotor were then conducted at rotor speeds of 20, 40 and 60 Hz. (i.e., rotor tip speeds of 4.9, 9.7 and 14.6 m/s). The data are shown in Figures 31, 32 and 33 respectively. As noted previously, the negative value of Δp_R at $V_S = 0$ reflects the pumping effect of the rotor (R). The data are shown in Table 5 along with the measured rotor speed, and they show that the pumping effect is roughly proportional to the square of the rotor speed. This is consistent with the assumption that the velocity imparted by the rotor to the fluid is proportional to the rotor tip velocity.

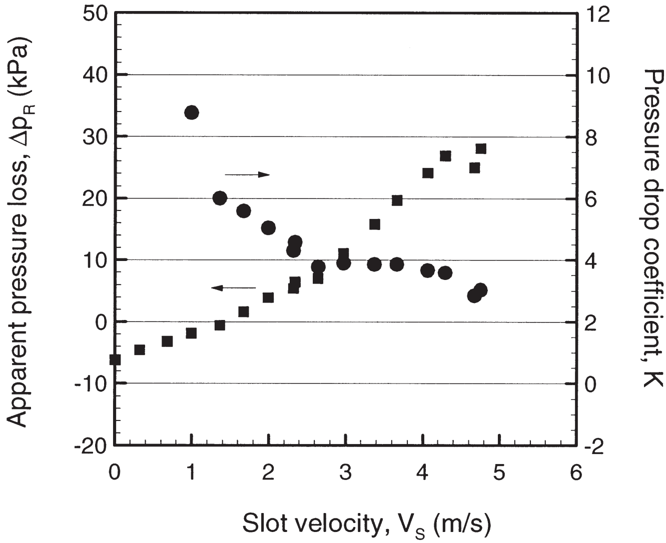

Figure 31 Pressure loss across screen plate (motor speed = 20 Hz).

Table 5 Effect of rotor speed on pumping effect (*R*).

Motor Freq. (Hz)	*Rotor Speed* (rev/min)	*Normalized Speed*	(*Normalized Speed*)^2	*R* (kPa)	*Normalized R*
20	400[1]	1	1	6.2	1
40	780	1.95	3.8	22.3	3.5
60	1140	2.95	8.1	46.0	7.4

[1]Note: Rotor speed (20 Hz) increased to 500 rev/min at high flow rates through the screen.

Values of *K* were determined from the values of Δp_S according to equation 1. Figures 31 to 33 all show evidence of the descending-constant form seen previously for the CFD and flow channel results. The hydraulic resistance of the screen plate increases with increases in rotor speed (i.e., increased upstream velocity), which is also consistent with the findings of the CFD and flow channel studies. As in the more fundamental studies, the data tend towards a single curve (Figure 34) when the normalized pressure drop is plotted against the normalized slot velocity. For these calculations, upstream

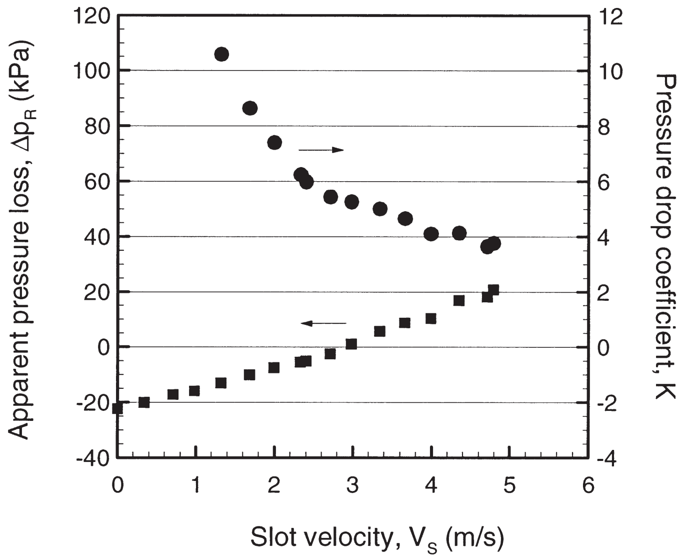

Figure 32 Pressure loss across screen plate (motor speed = 40 Hz).

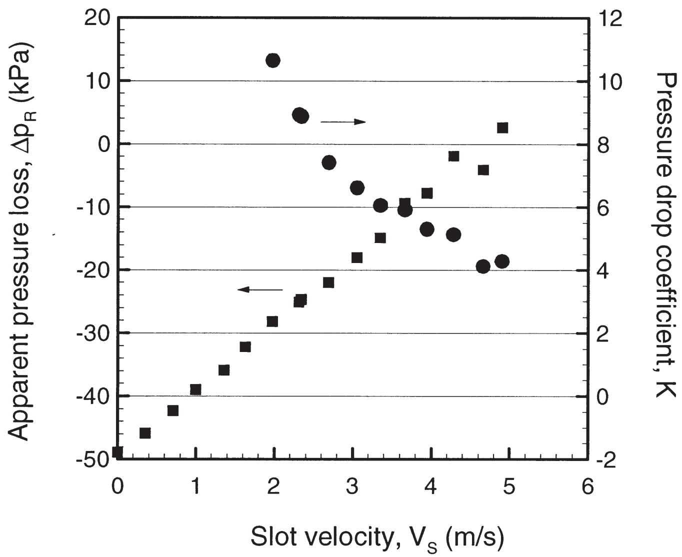

Figure 33 Pressure loss across screen plate (motor speed = 60 Hz).

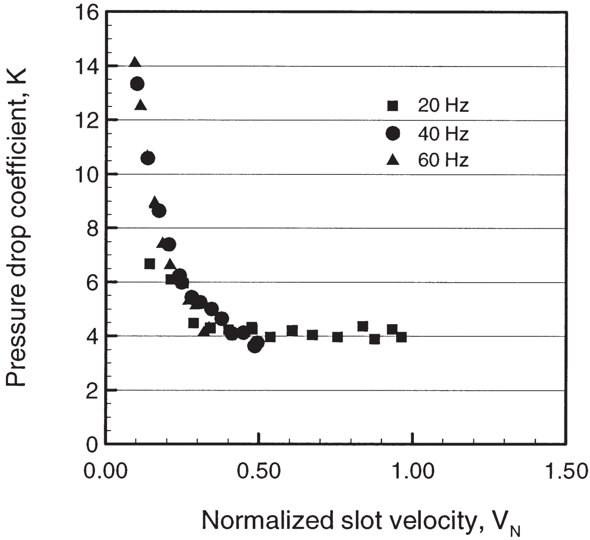

Figure 34 Pressure drop coefficient for pilot plant screen.

velocity was estimated as 85% of the rotor tip speed. The value of K at $V_N = 0.5$ is approximately equal to 4 according to the data in Figure 34. This compares closely to the values of K determined from the CFD and flow channel studies, which were 3.9 and 3.8 respectively for a step-step contour with $w_C = 1$ mm and $d_C = 1$ mm (see Figures 15 and 23).

One factor that was not considered in the above analysis was the effect of pulsations induced by the rotor. These represent a significant difference between the pilot plant tests and the flow channel studies. The form of these pressure pulses and their expected influence on hydraulic resistance is considered in detail in Gooding [39]. The conclusion was that pulses increase the apparent hydraulic resistance, especially at low values of V_S. However, for $V_N = 0.5$ and with a rotor speed of 60 Hz, the increase is less than 10%.

The additional influence of pulp suspensions was also examined in this study, and the results are shown in Figures 35 and 36. Even with pulp, the form of the K-V_S relationship still retained the descending-constant form observed in previous tests. The presence of pulp, however, caused a substantial increase in the value of K, doubling flow resistance, for example, from 10 to 20 at $V_S = 2$ m/s. A similar effect was seen in the flow channel tests (Table 3) where K increased by a factor of 1.3 at $V_S = 1.9$ m/s and by a factor of 2.3 at

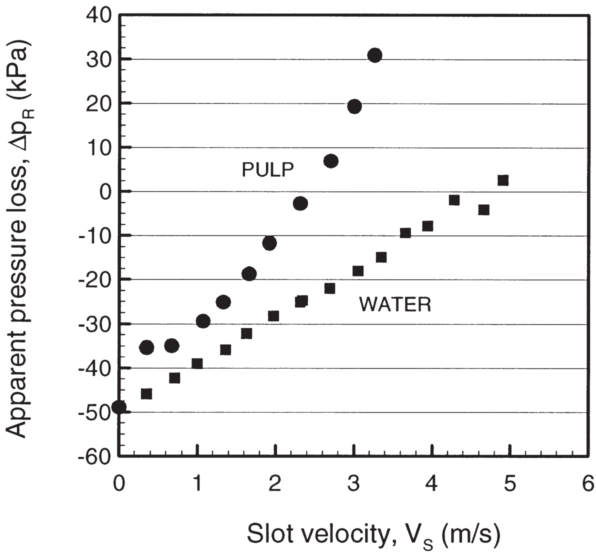

Figure 35 Pressure loss for pulp flow through pilot plant screen.

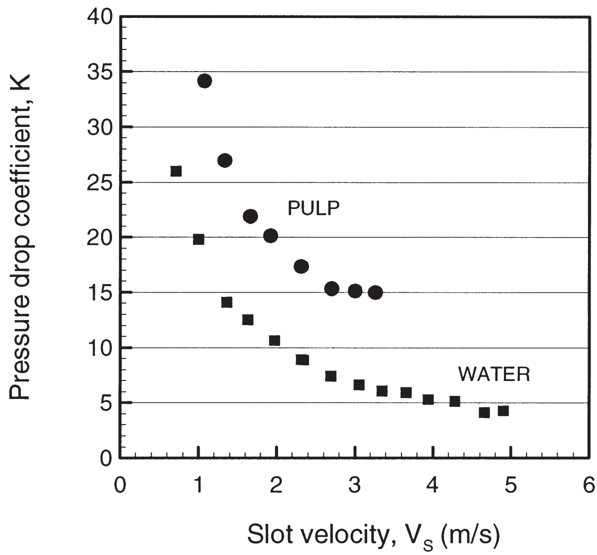

Figure 36 Pressure drop coefficient for pulp flow through a pilot screen.

$V_S = 2.9$ m/s because the fibre accumulation filled about half of the slot. There are substantial differences between the flow channel and pilot plant tests, including that the slot was smooth in the flow channel test and contoured in the pilot plant test, and that the differences in feed consistency would be expected to change to character of the fibre accumulation. The good agreement between the values of K may be somewhat fortuitous. At the same time, it would appear that these series of tests have represented and elucidated some of the key factors that determine flow resistance in pulp screens. As found in the flow channel studies, the contributions of simple hydraulic resistance and fibre accumulations are of roughly equal significance.

SUMMARY AND CONCLUSIONS

This study has provided a unique and methodical assessment of the pressure drop coefficient (K) for screen cylinders in pulp screens. It assessed the influence of factors related to the flow, plate geometry and pulp on K, and provided a framework to relate the findings of fundamental (CFD and flow channel) studies to the performance of industrial pulp screens.

CFD analysis showed that the relationship between K and the normalized slot velocity (V_N) could be characterized by two regimes: one where K decreased rapidly with V_N (descending regime), and the other where K is constant (constant regime). Examination of the flow patterns revealed that for smooth slots, there was a vortex on the upstream side of the slot that diminished in size in the descending regime. The flow then approached a pattern that was relatively unaffected by further increases in V_N (constant regime). Screen contours were found to reduce K, but the effect of a contour was dependent on the value of V_N. At low values of V_N (below about 0.3) the presence of a contour actually caused K to increase relative to the value for a smooth slot. Likewise, the influence of contour dimensions was more significant than indicated previously. For a step-step style of contour and $V_N = 0.5$, the optimal contour for hydraulic resistance had a depth of 0.25 mm and step-width of 0.5 mm. An increase in the contour depth to 1 mm caused K to double and to exceed the value for a smooth slot. The simple presence of a contour is not sufficient to cause a reduction in K.

Flow channel tests validated CFD findings, and good agreement with CFD was obtained in terms of the actual values of K, the form of the K-V_N relationship, and optimal dimensions of the step-step contour geometry. The flow channel tests found that multiple, closely-spaced slots tended to reduce K slightly. A step-slope contour design led to lower values of K than a step-step design. Most significantly, fibre accumulations that filled about half of the slot caused K to increase by a factor of 2 to 3. This indicates that fibre accumulations have a significant effect on flow resistance, but the hydraulic resistance due to simple water flow is also significant.

Tests of hydraulic resistance using an industrial pulp screen in a pilot plant yielded good agreement in terms of the specific values of K, the form of the K-V_N relationship, and the effect of pulp on K. In particular, the presence of pulp caused the value of K to increase by a factor of 2 at an aperture velocity of 2 m/s. The measured pressure drop across a screen was significantly affected by the pumping effect of the screen rotor, and losses from flow through the screen housing, but these could be measured independently from the resistance of the screen plate apertures and discounted.

A larger message of this work is that while screen contours can substantially increase screen capacity, their ability to reduce K is highly dependent on contour dimensions and local flow conditions. The simple presence of a contour does not guarantee the elimination of the slot vortex and the reduction of resistance. Pulp fibre accumulations have a more significant influence on K than any other factor. The influence of particular contour designs and dimensions, as well as different fibre types and consistencies, must be established.

This work has shown how CFD, flow channel tests and pilot plant trials can be combined to elucidate the factors that determine the flow resistance of screen plate apertures. While a number of questions have been answered, others have simply become better defined. Chief among the remaining questions is the need for a precise understanding of how contours reduce the tendency for fibre accumulations to initiate and grow. There is a need for a more detailed understanding of how flow reversals induced by the rotor affect apparent resistance. By building on this study, future work can create an increasingly comprehensive understanding that is essential for the use of ever-smaller screen slots.

REFERENCES

1. Thomas, A. S. W. and Cornelius, K. C., "Investigation of a laminar boundary-layer suction slot", *AIAA J.*, **20**(6): 790–796 (1982).
2. Boettcher P. C., "Results from a new design of contoured screen plate", *Proc. 1986 Tappi Pulping Conf.*: 279–283.
3. Frejborg, F., "Profile screens improve TMP system efficiency and increase pulp quality", *Pulp and Paper*, **61**(6): 99–101 (1987).
4. Hooper, A. W., "The screening of chemical pulp", *Pulp and Paper Manufacture*, 3rd ed., vol. 5, ch. 12, TAPPI/CPPA (1989).

5. Oosthuizen, P. H., Chen, S., Kuhn, D. C. S. and Whiting, P., "Fluid and fibre flow near a wall slot in a channel", *Proc. 1992 CPPA Tech. Sec. Ann. Mtg.*, B49–52.
6. Halonen, L., Ljokki, R. and Peltonen, K., "Improved screening concepts", *Proc. 1989, Tappi Pulping Conf.*, 61–66.
7. Gunther, J., "Calculation of flow patterns in the entry region of various contoured screen slots using the finite element method", M.A.Sc. Thesis, Technische Hochschule Darmstadt (1992).
8. Yu, C. J. and DeFoe, R. J., "Fundamental study of screening hydraulics. Part 1: Flow patterns at the feed-side surface of screen baskets; mechanism of fibre-mat formation and remixing", *Tappi J.*, **77**(8), 219–226 (1994).
9. Tangsaghasaksri, W., "Uber die sortierung von fasersuspensionen mittels geschlitzter siebe", Ph.D. Thesis, Technische Hochschule Darmstadt (1994).
10. Yu, C. J., Crossley, B. R. and Silveri, L., "Fundamental study of screening hydraulics. Part 3: Model for calculating effective open area", *Tappi J.*, **77**(9), 125–131 (1994).
11. Gooding, R. W. and Kerekes, R. J., "The motion of fibres near a screen slot", *J. Pulp Paper Sci.*, **15**(2): 59–62 (1989).
12. Kumar, A., *Passage of fibres through screen apertures*, Ph.D. Thesis, University of British Columbia (1991).
13. Julien Saint Amand, F. and Perrin, B., "Screening: Experimental approach and modelling", *Proc. 1998 Tappi Pulping Conf.*, 1019–1031.
14. Hacker, M. P. and Presley, R. L., "Mill experiences – aerodynamic rotor and profile slotted cylinders provide more efficient, higher capacity screens", *Proc. 1995 Tappi Pulping Conf.*, 657–663.
15. Mackie, D. M., Frith, M. D., Costantino, J. and Parker, S. M., "Low-medium consistency (4% consistency) screening", *Proc. 1990 CPPA Tech. Sect. Ann. Mtg.*, A305–A311.
16. McCarthy, C., "Factors affecting pressure screen performance", *Proc. 1987 Tappi Eng. Conf.*, 355–361.
17. McAndie J. L., "Versatility of pressurized pulp screen proven by mill experience", *Pulp and Paper*, **41**(32): 28–30 (1967).
18. Fredriksson, B., LeBlanc, P. E. and Goldenberg, P. H., "The Beloit S-Screen. A new concept for high consistency screening", *Proc. SPCI 87*, 1069–1081 (1987).
19. Goldenberg, P. H., "Recent developments in screening", *Proc. 1989 Tappi Pulping Conf.*, 73–75.
20. Travers, C. S., "Mill operating experience with a Beloit S-Screen", *Proc. 1988 CPPA Tech. Sec. Ann. Mtg.*, B255–B267.
21. Karvinen R. and Halonen L., "The effect of various factors on pressure pulsation of a screen", *Paperi ja Puu*, **66**(7): 80–83 (1984).
22. Wikstrom, T. and Fredriksson, B., "Hydrodynamics in a pressure screen: Consequences on the separation process", *5th Research Forum on Recycling Preprints*, 197–202 (1999).
23. Fredriksson, B., "Evaluation of apparatus and systems for screening mechanical pulp", *Svensk Papperstidning*, **87**(12): 94–98 (1984).

24. Hoydahl, H. E., “Practical and theoretical aspects of groundwood screening”, *Norsk Skogindustri*, **27**(9): 253–258 (1973).
25. Meinecke, A., “Development of a pressure screen for the screening of groundwood and chemical pulp”, *Wochenbl. fur Papierfabr.*, **106**(9): 333–336 (1978).
26. Hooper, A. W., “A comparison of slots and holes in the screening of mechanical pulp”, *Proc. 1987 CPPA Tech. Sect. Ann. Mtg.*, A249–A256.
27. O’Brien, M. J., “Groundwood secondary screening with the Centriscreen”, *Pulp and Paper Can.*, **63**(6): T311–T316 (1962).
28. Rautalahti, P., “Screening and reject refining in Kirkniemi mill”, *Proc. Symp. Mech. Pulp*, 137–144 (1970).
29. Martin, A. C., “Screen operation and maintenance”, *Pulp and Paper Manufacture*, 3rd ed., vol. 2, ch. 15, TAPPI/CPPA (1983).
30. Hourula, I., Kortela, U., Ahnger, A. and Hautala, J., “Fewer cascade connections, pumping and control loops in screening plants utilizing new technique”, *Proc. 1996 Tappi Recycling Symposium*, 435–442.
31. Walmsley, M. and Weeds, Z., “Flow characteristics of eucalyptus pulp suspensions in a pressure screen with 1 mm hole apertures”, *Proc. APPITA Ann. Conf.*, 271–278.
32. Torsten Paul, S., Duffy G. G. and Chen, X. D., “Viscosity control – A new way to improve pressure screen performance”, *Tappi J.*, **83**(9): 61 (2000).
33. Martinez, D. M., Gooding, R. W. and Roberts, N., “A force balance model of pulp screen capacity”, *Tappi J.*, **82**(4): 181–187 (1999).
34. Sobey, I. J., “Laminar boundary-layer flow past a two-dimensional slot”, *J. Fluid Mechanics*, **83**: 33–47 (1973).
35. Dewynne, J. N., Howison, S. D., Ockendon, J. R., Morland, L. C. and Watson, E. J., “Slot suction from inviscid channel flow”, *J. Fluid Mechanics*, **200**: 265–282 (1989).
36. Anderson, D. A., Tannehill, J. C. and Pletcher, R. H., *Computational Fluid Mechanics and Heat Transfer*, Hemisphere (1984).
37. Fletcher, C. A. J., *Computational Techniques for Fluid Dynamics*, 2nd ed., Springer-Verlag (1991).
38. Patankar, S. V., *Numerical Heat Transfer and Fluid Flow*, Hemisphere (1980).
39. Gooding, R. W., *Flow resistance of screen plate apertures*, Ph.D. Thesis, University of British Columbia, Vancouver (1996).
40. Amtec Engineering, *INTEC Ver. 1.1 User’s Manual*, Amtec Engineering Inc., Bellevue, WA (1993).
41. Roberson, J. A., and Crowe, C. T., *Engineering Fluid Mechanics*, 3rd ed., Houghton Mifflin (1985).

Transcription of Discussion

THE FLOW RESISTANCE OF SLOTTED APERTURES IN PULP SCREENS

R.W. Gooding[1], *R.J. Kerekes*[2] *and M. Salcudean*[3]
[1]CAE Forestry Systems, Pulp and Paper
[2]Pulp and Paper Centre, University of British Columbia
[3]Department of Mechanical Engineering, University of British Columbia

Kari Ebeling UPM-Kymmene Corporation

Based on your computational fluid dynamics and the verification with plexiglass models, could you imagine that the screen should have more similarity to the formation of the sheet; i.e. you should accelerate – and orient – the fibres to a certain velocity and then have slots in the same direction as the main velocity and try to suck the fibres without allowing them to form any network. This way you would get the rejects on the screen and the good ones through it. Then just scrape the rejects off the surface. Would this approach get rid of the extra resistance that the network provides?

Robert Gooding

I think there are opportunities to optimise the contours and slot geometries. One might not want to align the slots with the flow to avoid that sort of resistance because you create other problems with fibre accumulations, but I certainly think one can optimise the contour shape. It is the business of floc dispersion and that problem I'd like to take on myself. This involves looking at how flocs break up upstream of the apertures, how fibres deposit on the edge of the aperture entry and; whether full flocs come into the slot or discrete fibres. I think that is critical to understanding screens and allowing smaller apertures to work well.

Peter Herdman Arjo Wiggins

In the review paper by Dr Julien Saint Amand, we saw some diagrams which tend to imply that the size of particles separated by a screen would depend somewhat on the inlet geometry. Do you think that there is any sort of correlation between the increased flow rate that you've seen with certain geometries and the ability to pass larger particles through a particular geometry?

Robert Gooding

This is an area where we don't have enough data. We have a sense that higher velocities tend to drive through stickies and conformable particles but I think that the debate remains. There is also debate on the effect of the pressure pulsations on contaminant passage. Recent work has considered the back flush effect and how you can not only contour the feed side of the slot but contour the accepts side too. Thus when the rotor comes by and creates a suction pulse, it draws more fluid than one would expect. That can also be part of what is controlling stickies passage, whether the contaminant is being pushed through by the large pressure differential; high velocity.

Jean-Claude Roux EFPG

You use, by computational fluid dynamics, the k-ε model with parameters inside. Did you use the results from your experimental trials to re-adapt these parameters or were they OK in the beginning?

Robert Gooding

We used the second case. We estimated the turbulence levels and chose k-ε parameters based on typical values for water in a flow channel. What we attempted in the flow channel work was to create a fully developed flow upstream of the aperture. Thus we were able to assume at typical parameters for that temperature and viscosity of water flowing at that particular velocity.

Jean-Claude Roux

It is very interesting, it means that only with water we can describe some effects related to the K parameter you describe versus the slot velocity.

Robert Gooding

It's a good place to start, yes. But I think while k-ε models give us a useful tool to work with, there is much more to do in terms of optimising of the contours and understanding the fibre motion and floc dispersion at the slot entry.